HIGH TEMPERATURE FASTENER FATIGUE

by

James Mark Hobbs

A thesis submitted to the faculty of
The University of Utah
in partial fulfillment of the requirements for the degree of

Master of Science

Department of Mechanical Engineering

The University of Utah

August 2010

The University of Utah Graduate School

STATEMENT OF THESIS APPROVAL

The thesis of **James Mark Hobbs**

has been approved by the following supervisory committee members:

Daniel O. Adams	, Chair	**3/18/10**
K. L. DeVries	, Member	**3/18/10**
Ken Monson	, Member	**6/4/10**

and by [redacted] , Chair of

the Department of **Mechanical** [redacted]

and by Charles A. Wight, Dean of The Graduate School.

ABSTRACT

This work was commissioned in response to high temperature fatigue failures in a bolted connection that rotates at high speed. There was concern about the loss of preload in the fasteners at high temperature due to thermal expansion in the fasteners. A substitution of fastener material was made and the failures ceased.

The two major focuses of this work are preload and fatigue behavior of fasteners. Preload can be determined by many different methods with varying degrees of accuracy. After investigating and testing different methods of measuring preload, a new method is proposed herein that is application specific, eliminating the need for many of the assumptions common to other methods. Modeling and testing also confirmed that the preload of original fasteners was being completely lost at elevated temperature, and the new fasteners were maintaining preload. Fatigue testing was also performed on the fasteners to determine the fatigue behavior of the fasteners and the effects of temperature on fatigue life. It was determined that maintaining preload at temperature is the most important factor on fastener life in this application, and that temperature does not have great effect over the temperature range considered.

TABLE OF CONTENTS

ABSTRACT iii

LIST OF FIGURES vi

LIST OF TABLES viii

ACKNOWLEDGEMENTS ix

1: INTRODUCTION 1

Nomenclature for Bolted Connection 2

2: LITERATURE REVIEW 4

A-286 4
I-909 7

3: DYNAMIC/LOADING ANALYSIS 8

4: PRELOAD DETERMINATION 10

Fastener Preload Measurement Methods 10
Mechanical Measurement: Dial Indicator 12
Spring Constant Determination 13
Stretch Measurements 18
Bending Calibration 20
Three-Point Bending Calibration 21
Eccentric Bending Calibration 22
New Method: Joint Strain Calibration 23
Calibration Data Collection 24
Finite Element Model for Strain Estimation 26
Strain Measurement at Nominal Torque 28
Calibration Method and Results 31
Method Applicability 32
Supporting Calculations 34
Conclusions 38

5: INITIAL FATIGUE TESTING 39

Fixture Design 39
Initial Room Temperature Testing 41
Initial High Temperature Testing 42
Results of Initial Tests 48

6: FINITE ELEMENT ANALYSIS OF TEMPERATURE EFFECTS ON PRELOAD 49

Solid Model 49
ANSYS Script File 50
Results of Finite Element Analysis 52

7: FINAL FATIGUE TESTING 55

Tensile Strength Testing 55
Fatigue Testing 56
Testing Results and Temperature Effects 57

8: CONCLUSIONS 60

Preload Determination/Behavior 60
Finite Element Model 60
Testing Approach 61
Fatigue Results 61
Cause of Failure 61
Design Methodology 62

APPENDICES

A: ANSYS CODE FOR TZM DISC MODEL 64

B: ANSYS CODE FOR PRELOAD TEMPERATURE EFFECTS 66

C: MTS TEST PROGRAM FOR FASTENER TENSILE TESTING 70

D: MTS TEST PROGRAM FOR FASTENER FATIGUE TESTING 75

REFERENCES 80

LIST OF FIGURES

1: Diagram of Bolted Connection 3

2: Frequency Domains in Fatigue Testing of Metals 5

3: Cutoff Frequency for Time Independence for A-286 6

4: Temperature Independence of A-286 Fatigue Life in Vacuum 6

5: Nomenclature for Equation 3 14

6: Spring Constant Fixture 15

7: Spring Constant Fixture in the 5 kip Instron 16

8: Extensometer Calibrator 17

9: Sample Load vs. Displacement Plot for Spring Constant Testing 18

10: Elongation Measurement Setup 19

11: Fixture for Fastener Stress Durability Tests 20

12: Load Path for Calibration Testing 25

13: Finite Element Mesh 26

14: X-Direction Strain of TZM Disc 27

15: Y-Direction Strain of TZM Disc 28

16: Joint Strain Measurement Setup 29

17: TZM Disc with Strain Gages 30

18: Example Calibration Chart 31

19: Effect of Wear on Preload 33

20: Variation in Preload by Location on TZM Disc 33

21: Block on an Inclined Plane 34

22: Test Setup for Coefficient of Friction Measurement 35

23: Preload Comparison 38

24: Preloading Test Fixture 40

25: 3.3 Kip Servo-Hydraulic Testing Machine 41

26: Oven before Refurbishment 44

27: Oven after Refurbishment 44

28: Water Jacket above Oven 45

29: Oven and Water Jackets Mounted on Machine 46

30: TZM Preload Fixture Calibration Data 48

31: Finite Element Mesh for Preload Model 50

32: Axial Stress in I-909 Fastener at 750 ºF 51

33: ANSYS Model of Preload vs. Temperature 52

34: Gap under A-286 Fastener Head 53

35: A-286 Fatigue Testing Results 59

36: I-909 Fatigue Testing Results 59

LIST OF TABLES

1: Spring Constant Test Results 18

2: Final Preload Results 32

3: Measured Coefficients of Friction between Surfaces 35

4: Ultimate Load Results from Tensile Testing 56

5: Fatigue Testing Results 58

ACKNOWLEDGEMENTS

I would like to thank Dr. Dan Adams for all of the great help and insight he provided during the course of this project. Jeff Kessler also deserves many thanks for all of the assistance in testing and for the use of his lab. Those that have contributed to the completion of this project include:

University of Utah

Dr. Daniel Adams, Advisor, Committee Member

Dr. Paul Borgmeier, Former Committee Member

Dr. K. L. DeVries, Committee Member

Dr. Ken Monson, Committee Member

Dr. Seubpong Leelavanichkul

Dr. Eberhard Bamberg

Jeff Kessler, Lab Manager

Client

Greg Andrews, Engineering Manager

Dr. Chris Lewis, Phd, Engineer

Ricky Smith, Engineer

Last of all, I would like to thank my wife Amy for all her love and support.

1: INTRODUCTION

Bolted connections are commonly used in applications where rotation of the assembly leads to fatigue loading. In such assemblies, fatigue failure in the fasteners may cause the destruction of the entire subassembly, loss of expensive equipment, and possible safety risks. This investigation focuses on a bolted connection that rotates at 110 to 150 Hz. The bolted connection is encased in a vacuum and attains an estimated temperature of 750 °F (400 ºC) when in use. Previous investigations have confirmed that the fasteners failed in fatigue (1).

The objectives of this research investigation are:

- Measurement of the preload developed in the fasteners during assembly of the bolted connection.
- Quantification of the difference between air and vacuum on the fastener fatigue life at room temperature and 750 °F (400 ºC).
- Quantification of the effect of elevated temperature on fastener fatigue life.
- A correlation between a simulated fastener assembly and individual fastener testing. The goal is to develop individual fastener testing that is representative of the assembly.
- Fastener fatigue data applicable to the intended application.
- A design process/methodology for future bolted joint designs for use in the intended application.

Nomenclature for Bolted Connection

It will be useful to establish nomenclature for the various components in the bolted connection and the materials. A diagram is shown in Figure 1.

Bearing: A rotary bearing with two races rotating about a common axis, creating a rotating cantilever. Constructed of tungsten tool steel with a Rockwell C hardness of 65.

Bearing stem: Also referred to as the *stem*. The component containing the inner races of the bearing. Referred to in finite-element modeling as WTS, short for tungsten tool steel.

Bearing flange: The flat area on the end of the bearing stem into which the fasteners thread.

TZM Disc: Also *disc*. The disc-shaped component that the fasteners secure to the bearing stem. Constructed of TZM, a molybdenum alloy.

A-286: A nickel-based superalloy used frequently in elevated temperature applications due to its favorable properties.

I-909: A low-expansion superalloy designed to have favorable strength properties at elevated temperature, while maintaining a CTE about half the magnitude of A-286. Trade name is Incoloy 909.(2) I-909 is a designation used herein for convenience.

Fasteners: A set of six 8-32 screws, arranged in a regular hexagon, that connect the bearing stem to the TZM disc. Fabricated from either A-286 or I-909.

Cantilevered mass: A mass of about 13 lbs (5.9 kg) that is hard connected to the TZM disc.

Bolted Connection: Also joint. The joint formed with the connection of the bearing stem to the TZM disc.

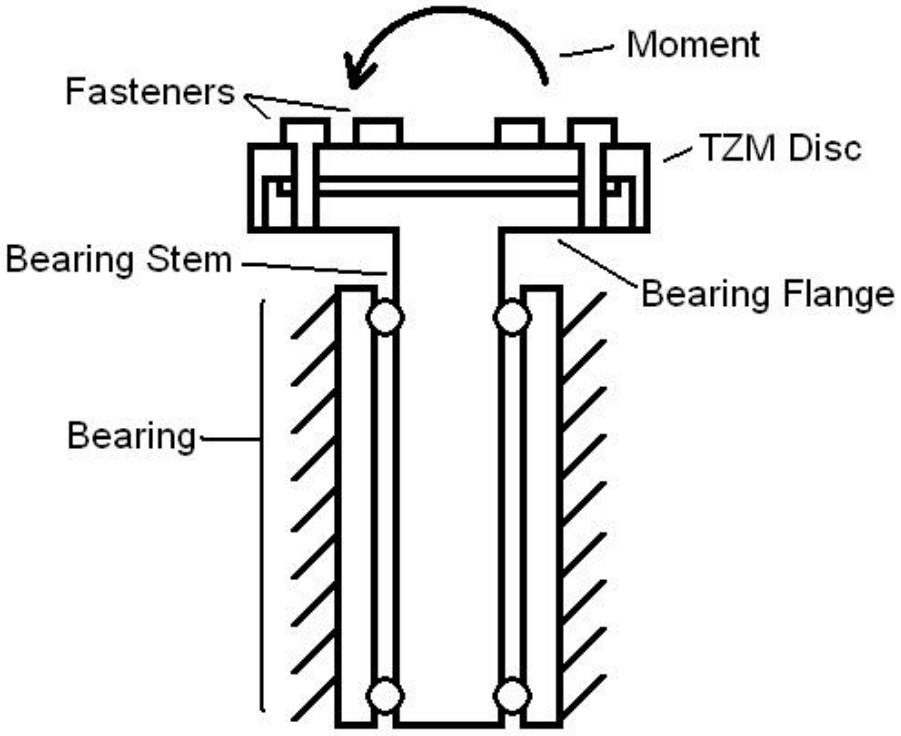

Figure 1: Diagram of Bolted Connection

2: LITERATURE REVIEW

A literature review was performed to gather information relative to the two fastener materials, their behavior in fatigue, and fatigue testing at elevated temperatures. Material concerning preload will be addressed in Chapter 4: Preload Determination. As A-286 is a common superalloy used in high-temperature applications, considerable information was found relating to its use in elevated temperature fatigue environments. Less information was found for I-909, as it is a more recently developed alloy that is less widely used.

Of primary concern was the ability to test in an air environment, despite the fact that the fasteners are enclosed in a vacuum while in service. Testing in air would greatly simplify the environmental chamber setup and would allow for convective heating.

A-286

Coffin (3) did much work in high temperature fatigue of A-286 and some related alloys. He determined that fatigue behavior in many metals has three frequency domains. These domains are termed, in order of increasing frequency, material and environment sensitive, environment sensitive, and time independent. In this highest frequency domain, the testing frequency has no effect on the life of the component. This is because cracks that may form cannot be accelerated in their growth by corrosion caused by an air or other environment, because they are not open long enough. In a vacuum, the two higher frequency domains are equivalent because there is no environment to accelerate

crack growth. If testing is kept above the cutoff frequency of the time independent regime, air and vacuum results converge, as seen in Figure 2. It was determined that for A-286 this cutoff frequency is 1000 cycles per minute, or about 17 Hz, as seen by the convergence of lines in Figure 3.

It was also determined that in a vacuum, fatigue testing of A-286 at 20 ºC (68 ºF) and 593 ºC (1100 ºF) showed no significant difference. In Figure 4, this can be seen as the circles and triangles lie on the same line. It was not initially expected that fatigue behavior would be independent of temperature. Temperature independence may prove significant in this project by decreasing the amount of fatigue testing to be performed. If testing in a vacuum shows no effect of temperature, this may also be the case in the environmentally insensitive frequency domain; making testing unnecessary at intermediate temperatures between room temperature and the 400º C elevated test temperature.(3)

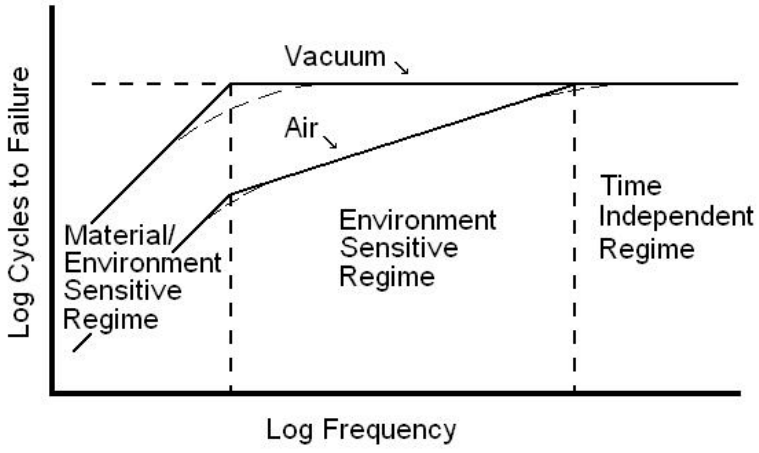

Figure 2: Frequency Domains in Fatigue Testing of Metals

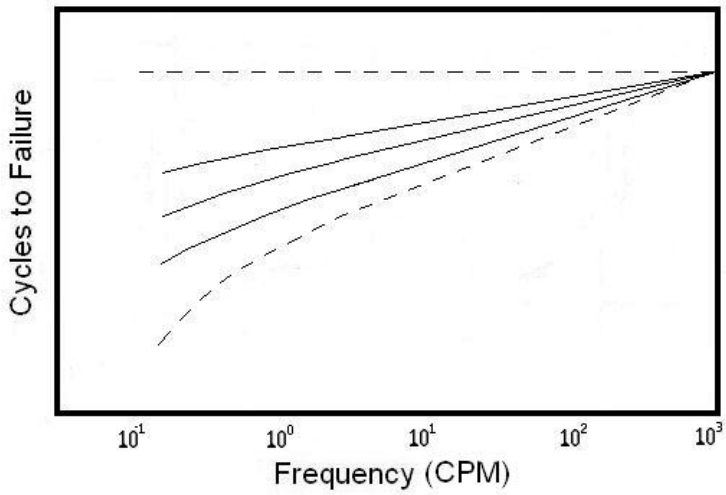

Figure 3: Cutoff Frequency for Time Independence for A-286

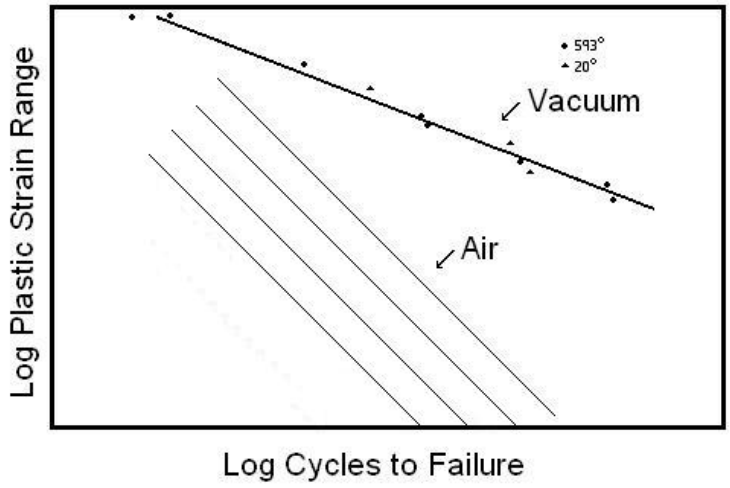

Figure 4: Temperature Independence of A-286 Fatigue Life in Vacuum

Coffin also did work to evaluate thermal-mechanical fatigue in A-286. Testing was performed to determine the effects of thermal cycling during each fatigue cycle, as opposed to a sustained high temperature. Temperature was changed at constant strain, and the strain was changed at constant temperature. It was determined that both in-phase (with the tensile portion of the cycle at elevated temperature) and out-of-phase (with the compressive portion of the cycle at elevated temperature) decreased the fatigue life as

opposed to a sustained temperature in the creep range. The in-phase testing had a decreased life due to grain boundary ratcheting, and the out-of-phase testing showed a decreased life due to grain boundary cavitation.(4)

I-909

A characterization study (2) performed during the development of I-909 was reviewed that discusses its improved properties. In order of obtain low thermal expansion characteristics, chromium is omitted from the Incoloy alloys. This omission causes the alloy to be vulnerable to Stress Accelerated Grain Boundary Oxygen embrittlement, or SAGBO. I-909 was developed specifically to maintain strength and thermal expansion properties and increase resistance to SAGBO. The addition of about 0.4% silicon significantly decreased the effects of SAGBO in the alloy, and achieved this without costly and time-consuming heat treatments. Fatigue crack growth rates measured for I-909 were nearly an order of magnitude lower than in the alloy I-903. This finding is important to this project, as testing in high temperature air could cause problems with SAGBO. Because SAGBO is significantly reduced in I-909, it is expected that any effects will be small and tend to make the data conservative.

3: DYNAMIC/LOADING ANALYSIS

The assembly that contains the bolted connection in question rotates around a gantry every 0.35 seconds, and rotates around its own axis at 110 Hz. The fasteners support a cantilevered load of 13 lbs. (5.9 kg) rotating about the gantry. The radius of rotation about the gantry is 27 inches (0.68 m). The radial acceleration is therefore:

$$r\omega^2 = 27\ in\left(\frac{2\pi}{0.35\ sec}\right)^2 = 8700\frac{in}{s^2} = 22.5g$$

Equation 1

As the gantry rotates, the radial acceleration passes from being aligned with gravity to being directly opposed to it. Thus, there is a ±1g ripple due to gravity, so the maximum acceleration the fasteners experience is 23.5 g. The maximum dynamic load reacted by the fasteners will be 23.5 times the static load under no rotation. The radial acceleration due solely to the 110 Hz rotation does not require a load in the fasteners to react it, so it is ignored. The dynamic acceleration does not consider vibration due to imbalance of the joint.

The force is reacted by six fasteners arranged in a circular pattern, holding the TZM disc onto the bearing stem. The cantilevered load produces a moment that tends to peel the TZM disc off of the bearing stem, with an axis of rotation about the bottom edge of the discs. To calculate the force in each fastener, the bending stress is calculated in each fastener and multiplied by its cross-sectional area. The bending stress is given by:

$$\sigma = \frac{M\,y}{I_{joint}}$$

Equation 2

where σ is the bending stress, M is the applied moment, y is the distance from the neutral axis, and I_{joint} is the moment of inertia calculated for the set of six fasteners. Despite the fact that the fasteners are rotating around the disc, I_{joint} is constant over time. As M is also constant, the stress only varies linearly in y. As the distance from the neutral axis in this case is a simple sine wave, so is the stress. The corresponding load ranges from 25 lbs (111 N) to 140 lbs (623 N), assuming constant stress across the fasteners.

There is also shear loading due to the cantilevered load. Each fastener would react 1/6 of the shear load, except that there are other load paths that preferentially take the load. The TZM disc has a lip around the outer edge that extends about ½ in. (12 mm) axially, so that the bearing stem slides into this area to contact the backside of the disc. There is also a frictional force between the bearing stem and TZM disc on the contact surface. It is common practice to ignore the shear loading in fasteners because of the high frictional forces between the clamped members. The shear load is thus ignored in the fasteners and the fastener loading is assumed to be purely axial due to the bending moment.

4: PRELOAD DETERMINATION

This chapter will discuss different preload measurement methods, and why their use in this application is problematic. A few of these methods were tested, and the results were not satisfactory. A new method is developed herein that successfully measured the preload in the small fasteners of this application.

Fastener Preload Measurement Methods

A major goal of this project is to accurately determine the preload developed in 8-32 x ½" fasteners constructed of A-286 and of I-909. The head of the fastener rests against a surface of TZM, which has unusual friction characteristics. Different methods of preload measurement are discussed below.

1. **Internally Gaged Fastener:** The company Strainsert (www.strainsert.com) installs a strain gage into the shank of the fastener. However, this service is not available for the small 8-32 fasteners used in this project. It also is not possible to use an allen wrench or screwdriver to tighten the fastener after a strain gage is installed due to wiring.
2. **Externally Gaged Fastener:** It may be possible to mount a strain gage to the exterior of a fastener. The A-286 fasteners do not have an unthreaded shank, so a space to mount the gage would have to be milled. This would change the apparent stiffness of the fastener. Another difficulty would be protecting the gage and routing the wires.

3. **Ultrasonic Measurement:** Precise length of a fastener can be determined by the time between ultrasonic pulses. The change in travel time of ultrasonic pulses can be used to find change in length, but only after calibration. Calibration is needed because the velocity of the ultrasonic waves is affected by temperature and stress level. The short length of the fasteners makes this unlikely to be effective.
4. **Mechanical Measurement:** The same as method 3, but the measurement method is mechanical. There is much less accuracy and precision in this method. This is typically performed with a micrometer or dial indicator. The use of a micrometer was explored prior to the beginning of this project without success.
5. **Load Washer:** A load cell is shaped as a washer and placed between the head of the fastener and the TZM. The smallest available from Omega Engineering (www.omega.com) is 0.35" (8.9 mm) thick and had an ID of 0.40" (10.2 mm), which is too large for this application. Additionally, the load washers are constructed of stainless steel, which will not preserve the friction effect of the fastener on TZM.
6. **Yield Sensing:** Calibrated equipment can sense an abrupt change in the torque gradient as the fastener is tightened, indicating yield. However, this method can only be used to tighten fasteners to yield, so it is not useful for measurement of preload due to a given torque.
7. **Bending Calibration:** The fastener is tightened down, causing a deflection in the surface against which the head rests. A testing machine is used to apply a load onto the deflected surface until the fastener is unloaded. The load on the machine

is approximately the preload developed in the fastener. The difficulty is in setting up the hardware to mimic the application.

A version of mechanical measurement was attempted first. Torque-to-failure data was provided by the client, and this was used to estimate the preload due to the nominal 40 in-lb (4.5 Nm) torque. Using the assumption that preload is linear with torque to failure; a simple proportion can be used with the failure torque, ultimate stress, and nominal torque. The A-286 fasteners failed at an average of 110 in-lbs (12.4 Nm), and the I-909 fasteners failed at an average of 65 in-lbs (7.3 Nm). Converting these values into load, the proportion gives a preload of 1018 lbs (4.5 kN) for A-286 and 1447 lbs (6.4 kN) for I-909.

There is serious doubt about the assumption that preload is linear with torque to failure, because stress and strain do not have a linear relationship through failure. Because the fasteners would be expected to have ductile behavior, this assumption most likely gives a preload estimate that is too high, so more direct means of measuring preload were pursued.

Mechanical Measurement: Dial Indicator

The next method utilized was to measure the stretch of the fasteners mechanically, with a dial indicator. A Starrett dial indicator graduated in 0.0001" (2.5 μm) increments was used to make the stretch measurements. A Stanley Proto torque wrench with a 200 in-lb (22.6 Nm) capacity graduated into 1 in-lb (113 Nmm) increments was used to apply torque to the fasteners.

Spring Constant Determination

In conjunction with stretch measurements, the spring constant of the fasteners, k_f, is required to convert stretch into preload. The spring constant was both calculated and measured experimentally. The calculation relies on the geometry of the fastener and the bulk material properties. The equation for k_f is as follows:

$$k_f = \frac{A_d A_t E}{A_d l_t + A_t l_d}$$

Equation 3

A_d - Unthreaded Area of Fastener

A_t - Threaded Area of Fastener

E – Young's Modulus

l_t – Threaded Effective Length = h + d/2 - l_d

l_d – Unthreaded Length

h – Top Flange Thickness

d – Nominal Diameter of Fastener

A diagram of some of these terms is found in Figure 5. Once the spring constant is known, a stretch measurement can be converted into a preload as follows:

$$F_i = \delta \cdot k_f$$

Equation 4

where F_i is the preload and δ is the stretch or deflection. The spring constant values were calculated to be 1278 kip/in (224 kN/mm) for the A-286 fasteners, and 1160 kip/in (203 kN/mm) for the I-909 fasteners.

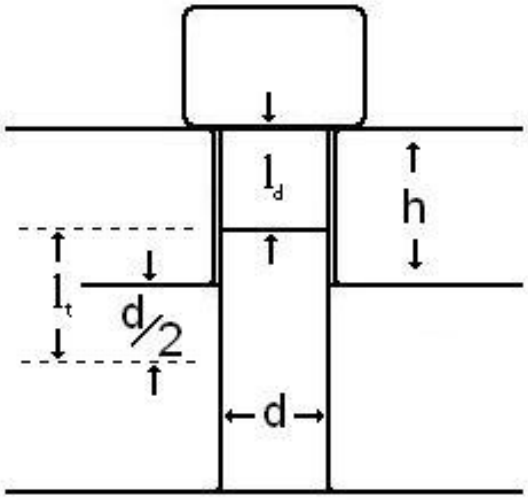

Figure 5: Nomenclature for Equation 3

The spring constant, k_f, was also determined experimentally. A fixture had to be designed that would allow the use of an extensometer on the fastener while loading in a test machine. A section of the solid model of the fixture is shown in Figure 6. The fixture consisted of two ½ in. (12.7 mm) diameter studs, each about an inch (25 mm) long. One was tapped for the 8-32 fasteners and also had a recessed area to allow for the extensometer. The other end had an axial blind hole large enough in diameter for clearance of the fastener heads. This hole extended nearly the entire length of the stud, leaving 1/8" (3 mm) at the bottom. There was also a through hole at the bottom, where the threaded portion of the fastener could protrude. The fixture was made of steel, and hardened, oil quenched, and annealed to a final Rockwell C hardness of about 40.

The fastener would be inserted into the blind hole, threaded portion first, and pushed until its head rested against the bottom surface and the threaded portion protruded from the bottom. The lower fixture piece would then be threaded onto the fastener, and

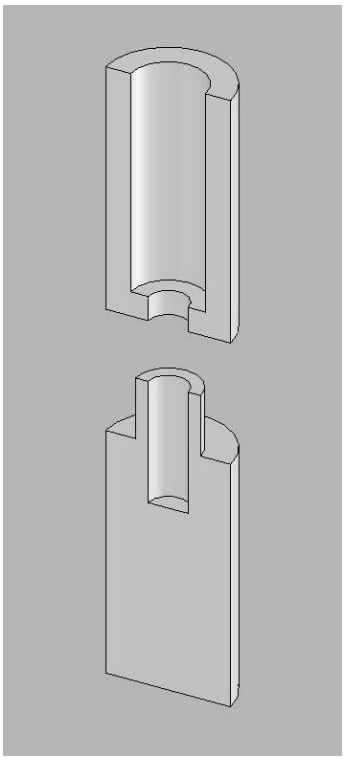

Figure 6: Spring Constant Fixture

this assembly mounted in wedge grips that attach to the testing machine. The extensometer was then fitted to the small threaded portion of the fastener between the fixtures. The fixture can be seen mounted in the Instron 4303 tabletop test machine in Figure 7. Longer fasteners (0.7", 18 mm) were required for these tests, and were provided by the project sponsor.

The extensometer, MTS model 632.26C-20, required calibration. The calibration was performed with an Epsilon Extensometer Calibrator, model 3590, shown in Figure 8 with the extensometer attached. While mounted in the calibrator, the extensometer was connected to a National Instruments SCXI-1314 strain board. Then by applying known displacements with the digital micrometer in the calibrator, the extensometer was calibrated by entering in the appropriate constants into the Labview program set up to read strains.

Figure 7: Spring Constant Fixture in the 5 kip Instron

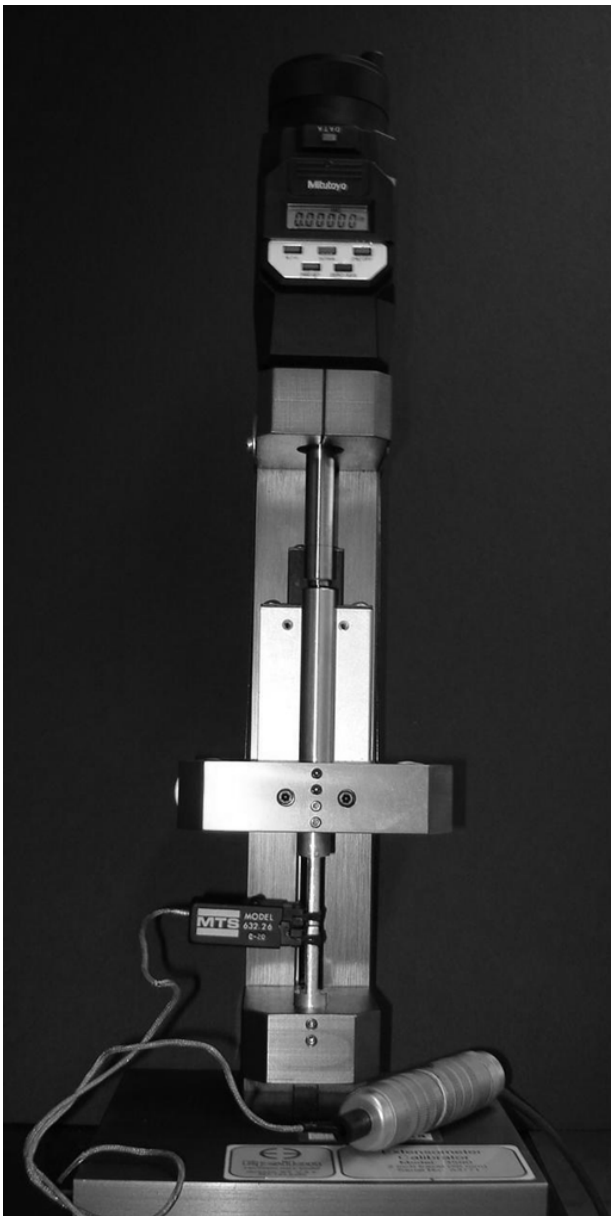

Figure 8: Extensometer Calibrator

Five tests were performed on each type of fastener. A sample plot of one of the tests is included in Figure 9. The deflection was recorded by the same National Instruments instrumentation that was employed during the calibration of the extensometer. The A-286 fasteners showed some scatter in spring constant values, but the average was near the calculated value. The I-909 measurements were significantly lower than the calculated value. Table 1 lists the results of the testing.

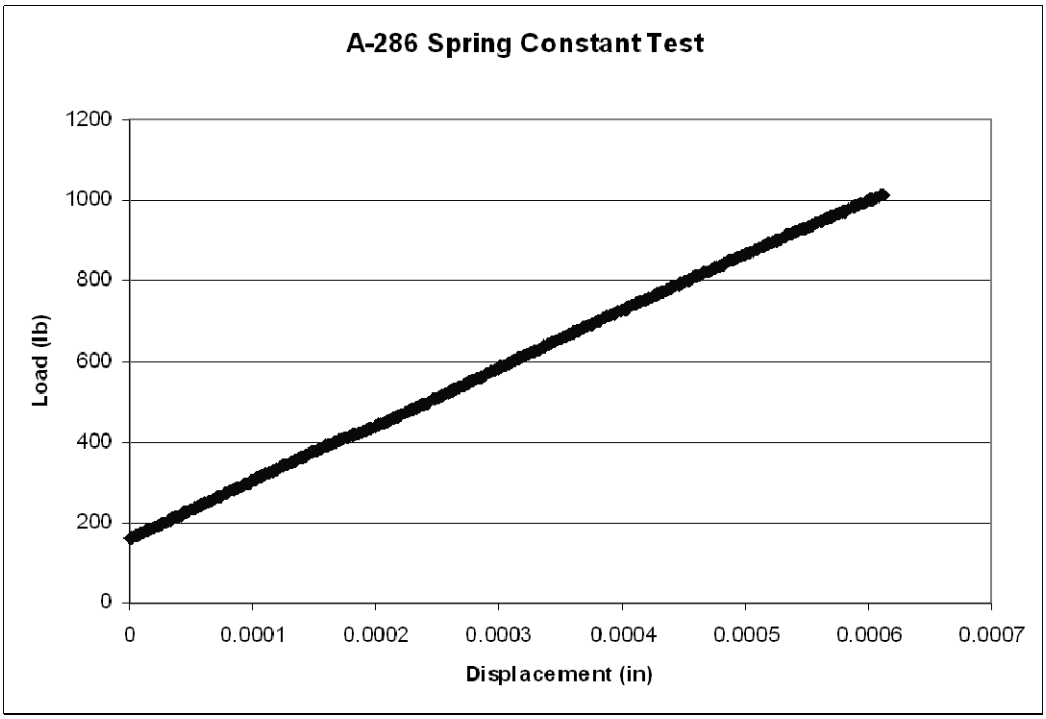

Figure 9: Sample Load vs. Displacement Plot for Spring Constant Testing

Table 1: Spring Constant Test Results

Fastener			Spring Constant
A-286	Mean	Kip/in	1311
	Std Dev	Kip/in	233
	CoV	%	17.7
I-909	Mean	Kip/in	794
	Std Dev	Kip/in	241
	CoV	%	30.3

Stretch Measurements

With the spring constant values determined, the stretch measurements had to be made. As shown in Figure 10, the bearing stem was secured in a vice, and the dial indicator held in position by a magnetic base stand, secured to the vice as well. The probe of the dial indicator was placed against the end of the fastener, and the fastener was tightened to the nominal torque of 40 in-lbs. Different tightening schemes were

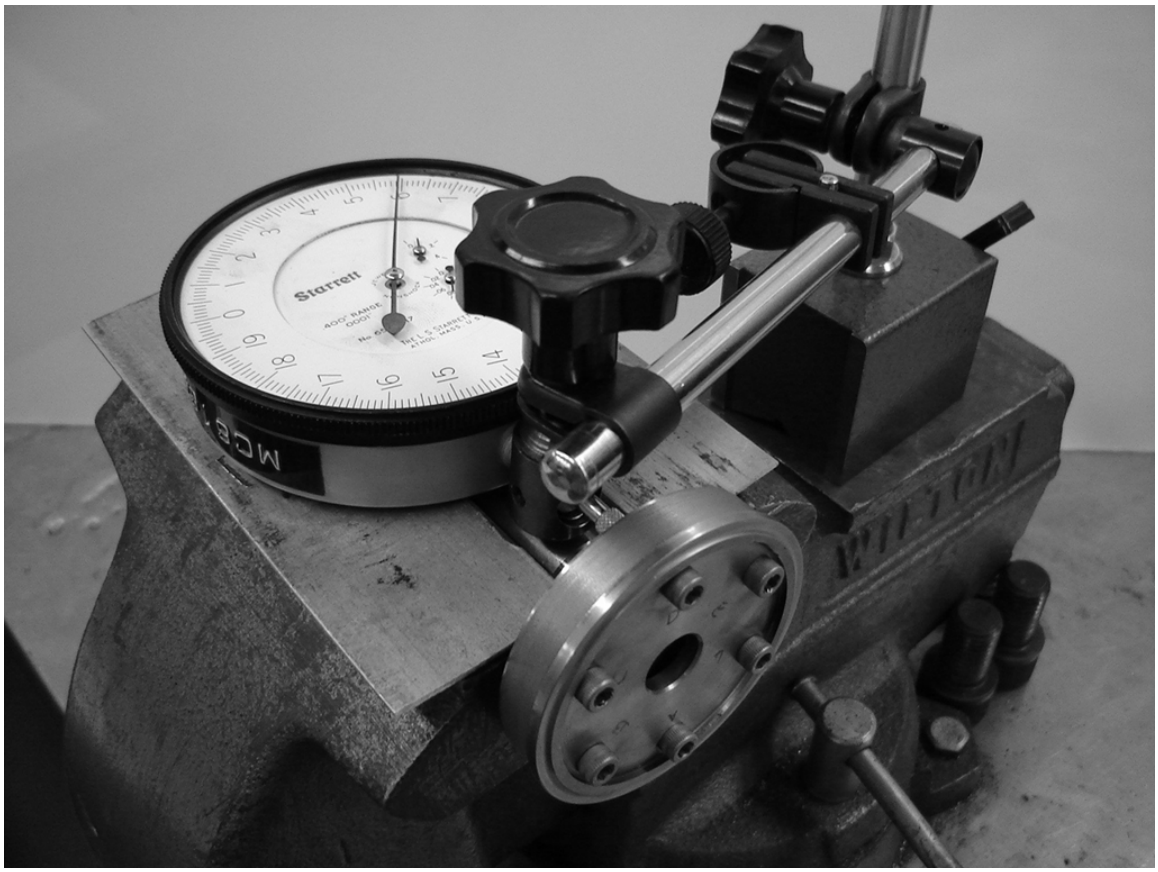

Figure 10: Elongation Measurement Setup

investigated. During some tests, all previously tightened fasteners were left at 40 in-lbs (4.5 Nm) during tightening. This procedure could show the effects of tightening order. During other tests, the dial indicator was left on one fastener while all of the others were tightened in turn, to investigate the effects of subsequent fasteners being tightened.

Dozens of stretch measurements were performed. The lowest stretch measurements obtained were about 1.5 thousandths of an inch (40 μm), and the largest about 3.5 thousandths (90 μm). If 3.5 thousandths were distributed as a uniform strain along the entire length of the ½" fastener, this would imply a 0.7% strain. That value of strain is certainly beyond yielding. As the fasteners were not yielding in the tests, it is certain that the setup of the dial indicator was measuring additional displacements aside

from the stretch of the fastener. Additional displacements would include settling of the TZM disc onto the bearing stem, and deflections due to the compliance in the magnetic base armature. Whatever the causes, no simple solution was identified to isolate the deflection of the fastener from the other deflections, so the method was abandoned.

Bending Calibration

The initial concept for this method came from a military test standard (5) used to load fasteners for stress durability tests. The basic setup is a beam supported above a large baseplate by a pair of dowel pins. The beam is loaded so that it deflects down toward the baseplate. A fastener is inserted through a hole in the beam and screwed into a threaded hole in the baseplate. The fastener is tightened, and as the load on the beam is removed, the fastener develops a preload to hold the beam in its deflected state. The basic fixture can be seen in Figure 11. It is noted that the deflection of the baseplate is ignored in the standard, and this deflection will introduce error into the deflection of the fastener. Despite errors in the actual standard, the general concept appears useful. Any calculations could be performed more rigorously than in the standard to yield more accurate results.

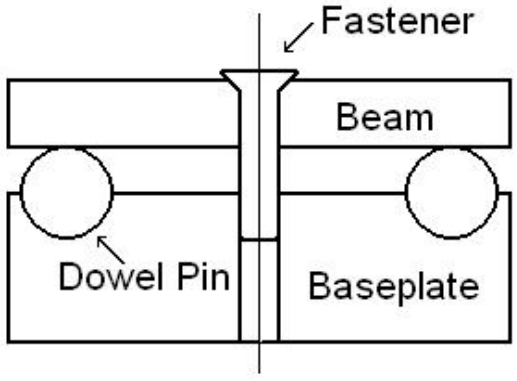

Figure 11: Fixture for Fastener Stress Durability Tests

It was desired that the test fixture consist of two ‘beams’, one constructed of TZM and another of tungsten tool steel, so as to preserve the materials of the intended application. These beams would be held apart by supports. The fastener would be used to clamp the two beams together. The preload developed would be measured in one of three ways. The first is to preload the fastener, and then replace the load applied by the fastener with a test machine until the fastener is unloaded, at which point the machine would read the fastener preload. The second is to produce measurable deflections in the beams which can be either analytically predicted or calibrated without the fastener applying the preload. The last method is to apply strain gages to the beams, and then calculate the corresponding load, again using analytical equations or a calibration.

Three-Point Bending Calibration

The geometry of the ‘beams’ needed to be worked out. The initial design phase utilized a three-point bend setup. It was desired that the beams be rectangular for simplicity of design, support setup, and ability to estimate deflections. As the beams were to be constructed from the TZM disc and bearing stem, the existing material constraints were:

- The span could not be greater than 1 inch (25 mm)
- The thickness of each beams was established
- The beams could not exceed their yield stress
- The combined thickness of the beams and deflections could not exceed 0.50 in. (12.7 mm)

It was desired that the deflections not exceed 0.05 in. (1.25 mm), which is the existing gap in the actual joint. The combined deflection (6) of the two beams is:

$$\delta = \frac{PL^3}{48E_1I_1} + \frac{PL^3}{48E_2I_2} = \frac{PL^3}{48(E_1I_1 + E_2I_2)}$$

Equation 5

where δ is the deflection, P is the load, L is the beam span, E is Young's Modulus, and I is the first moment of area. The bending stress equation for a simply supported beam of thickness t is the other controlling equation:

$$\sigma_i = \frac{PLt_i}{8I_i}$$

Equation 6

With the above constraints, the controllable geometric quantity was the width of each beam. In order to keep the relatively weak TZM below yield, the width had to be greater than the span, which certainly makes the beam equations invalid. It was then attempted to increase the thickness, but this did not give satisfactory results within the constraints. In trying to minimize stress, width, and thickness, it was determined that no combination of width and allowable thickness could prevent yielding in the TZM beam.

Eccentric Bending Calibration

The next attempt was to make the three-point bend setup eccentric, so that the load was not placed mid-way between the supports. The deflection has a maximum that is not at the load application point, so two deflections are calculated. The equations (6) are now more complex:

$$\delta_{max} = \frac{Pb(L^2 - b^2)^{3/2}}{9(\sqrt{3})EIL}$$

Equation 7

$$\delta_P = \frac{Pa^2b^2}{3EIL}$$

Equation 8

$$\sigma_i = \frac{P\left(\frac{L}{4} - \left(\frac{a-b}{2}\right)^2\right)t_i}{2I_i}$$

Equation 9

In these equations, *L* is still the length, and *a* and *b* are the lengths of the beam on either side of the load, *a* > *b*. With this additional degree of freedom, a solution was found that kept the stresses in the beams below yielding, but the geometry was extreme. The TZM beam was 0.465 in. (11.8 mm) wide, the steel beam was 0.15 in. (3.8 mm) wide, and the load was extremely eccentric. The need for a fastener hole in the steel beam also made the narrow width a problem. The steel beam would need to be made locally wider near the hole, changing the beam properties. The manufacture of such a setup would also be difficult, especially due to the extremely high strength of the steel. (Its hardness was measured to be a 65 on the Rockwell C scale.) The idea behind Bending Calibration was simplicity of design, and its final form proved to be too complicated to be useful.

New Method: Joint Strain Calibration

Due to the extreme difficulty in devising a geometric setup that could produce a sufficiently large deflection or strain, it was decided to measure the strain produced in the actual joint upon tightening of the fasteners. A single strain gage, a Vishay Measurements EA-13-125BZ-350, was applied to the surface of the TZM disc inward of one of the holes, oriented in the radial direction. The fastener was tightened partially, and a strain was produced that was sufficiently large to be seen despite noise. This informal

experiment was repeated several times to varying loads, and the strain appeared to have a linear relationship to torque applied.

It was decided that simply calibrating the joint itself was much simpler than designing a fixture to replicate the characteristics of the joint. This approach would preserve all of the physics of the actual problem. The frictional forces, materials, geometry, plate stiffness, and other factors would all be satisfied automatically.

There are two relationships to be determined: the torque-strain relationship, and the strain-preload relationship. Once both of these are known, it can be estimated what the nominal torque will produce as a preload. The torque-strain relationship is determined by tightening the fasteners to the nominal torque and measuring the strain produced. The strain-preload relationship is determined by calibrating the strain readings to the applied load, which is done on a testing machine.

Calibration Data Collection

In using this "measure and calibrate" method, it is important that the calibration reflects the same loading and support conditions as the measured quantity. In doing initial calibration tests, it was noticed that the results depended on the support and loading conditions. The manner in which the load is introduced into the fastener hole on the TZM disc and transferred out of the other end of the fastener hole in the bearing stem had to be made to match the conditions which a fastener would normally apply.

A ball bearing was initially used to introduce the load directly into the TZM disc. The joint was supported by a large steel block. Various setups were investigated until the final setup was determined. As seen in Figure 12, a ball bearing sits on the head of a

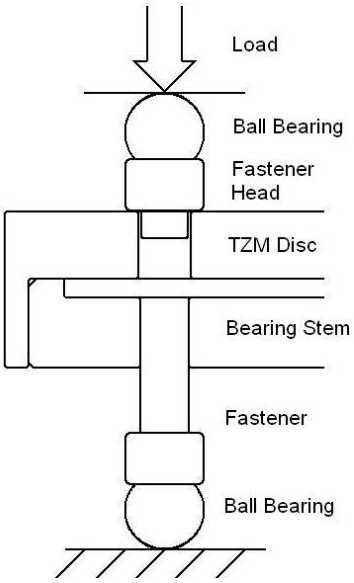

Figure 12: Load Path for Calibration Testing

sawed-off fastener that rests in the fastener hole of the TZM disc. Another fastener is threaded into the hole in the bearing stem such that its head protrudes from the bottom. That fastener head rests on another ball bearing, which has a direct path to ground through a large steel block. In this way, the load is introduced and exits the joint evenly. The joint is also loaded by the fastener head and threads as is it in service. The bearing stem was also inserted into a large hole so that the entire joint could not rotate on the ball bearings, but would remain vertical. It was also assured that this did not introduce a redundant load path. A strain rosette (Vishay Measurements EA-13-060RZ-120) was used with gages at 0, 45, and 90˚ to the radial direction to assure that the strain field produced by the fastener was well replicated by the calibration loading.

After determining that the best setup was found for the calibration tests, it had to be determined at what orientation the strain gage should be mounted to read the highest possible strain. The maximum strain that the rosette recorded was always in the 90˚ direction, which was not expected.

Finite Element Model for Strain Estimation

It was decided to make a finite-element model of the TZM disc to verify that the circumferential strains were larger than the radial strains. One half of the TZM disc was modeled in ANSYS, with the line of symmetry bisecting the hole that would be loaded. It was a 3-D model, as the loading is transverse to the plane of the disc. The load was placed as a pressure on the area normally covered by the fastener head, and the model was supported on the same area where the disc contacts the bearing stem on the reverse side of the disc. The mesh used in the model is shown in Figure 13.

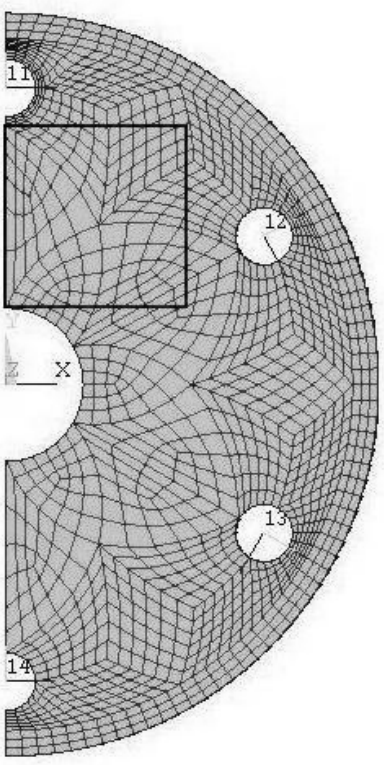

Figure 13: Finite Element Mesh

The strains in the X and Y directions of the surface elements at the location of the strain gage were compared. Plots of the X and Y direction strains for the area inside the square shown in Figure 13 are included in Figure 14 and Figure 15. From this model, it was determined that a 90˚ gage should read 2-5 times what an axial gage would read at that same location, depending on the size and placement of the gage. It was thus decided that a relatively small 90˚ gage would be placed inward of the fastener location to be calibrated. The gage must be small as there is a large gradient in the strain field, and thus a larger gage would read lower values because it covers a larger area around the peak strain.

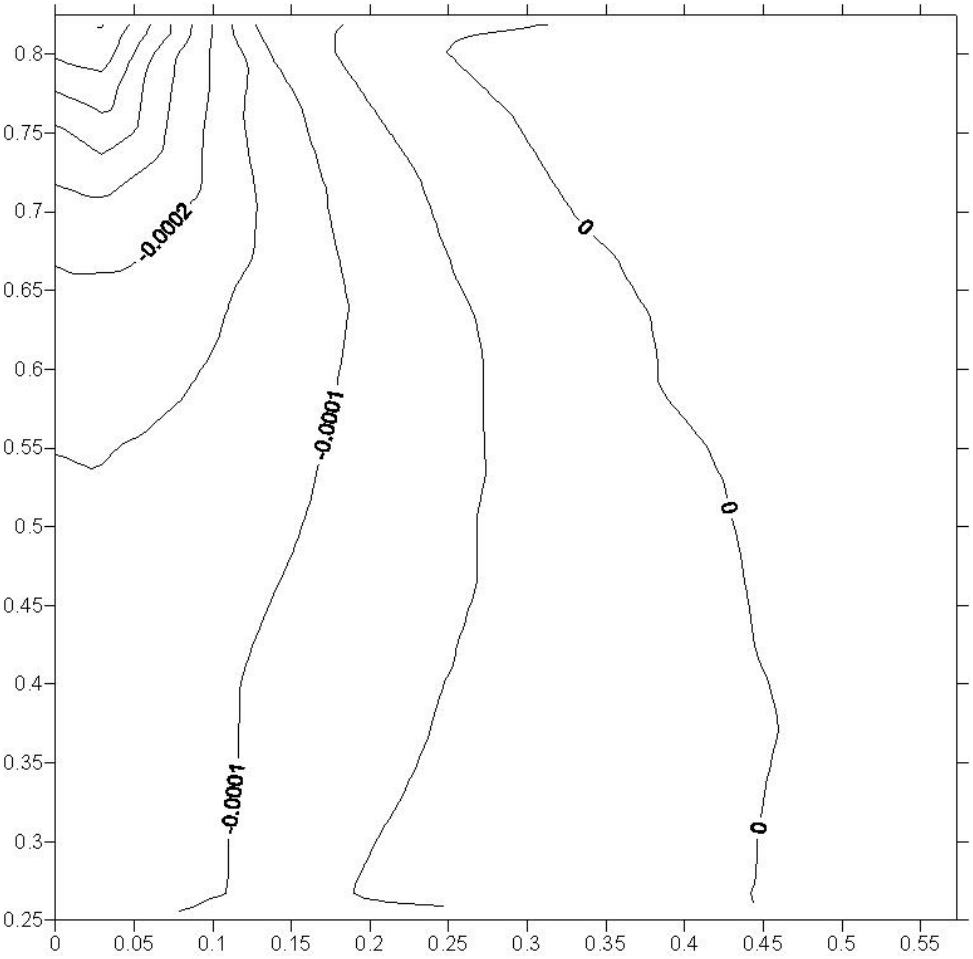

Figure 14: X-Direction Strain of TZM Disc

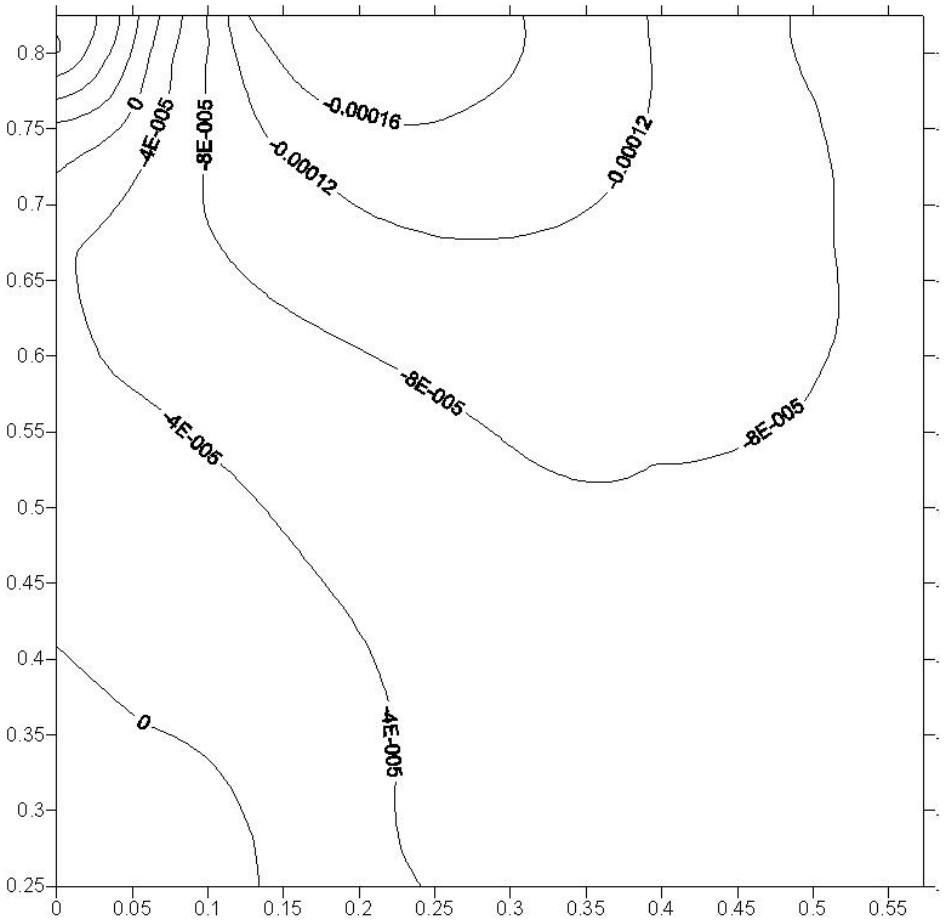

Figure 15: Y-Direction Strain of TZM Disc

Strain Measurement at Nominal Torque

To perform a "torque test," a fastener was inserted into a hole with a strain gage placed next to it. The strain gages were read using a Vishay Measurements Group P-3500 Strain Indicator and, if more than one were being read at a time, a Vishay SB-10 Switch and Balance Unit. The gage was zeroed out, and the torque then applied to the fastener. The strain was recorded, and then the fastener was loosened. The setup for taking these measurements is shown in Figure 16. The strain for the calibration tests was read using the same setup on the 5 kip Instron 4303 tabletop test machine as the extensometer readings in the spring constant tests.

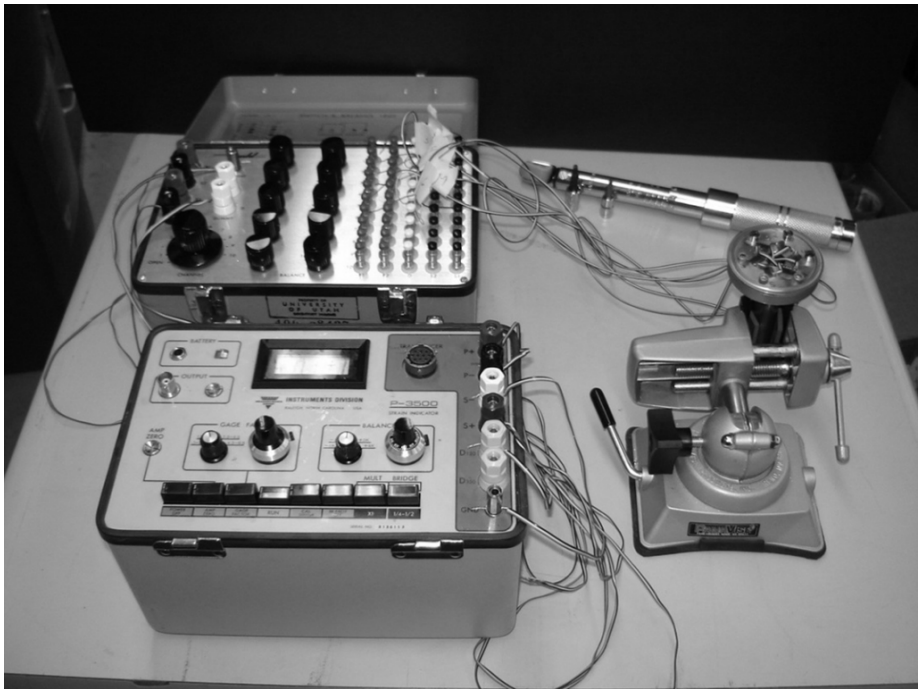

Figure 16: Joint Strain Measurement Setup

A comparison of results obtained using the Vishay and National Instruments systems was performed to assure that the strain measurements of each were comparable. A fastener was tightened while connected to one system, and subsequently loosened while connected to the other. These tests were performed four times. Results showed that the Vishay system read higher than the National Instruments system, but the average difference was less than 5%. This degree of correlation was deemed acceptable.

The original hole that was instrumented was used for various tests and was observed to have significant wear. The TZM surface appeared smoother underneath the fastener head, and the strain produced for a given torque changed over time. The torque applied to the fastener head is reacted by the frictional forces on the threads and underneath the fastener head. If the roughness of the surfaces were being changed, different normal forces (preload) would be required to react the same torque, explaining

the change in strain and corresponding preload. Thus, the issue of wear on the TZM surface and on the threads of the bearing stem merits attention. In the actual application fastener wear is not an issue since fasteners are not reused.

As the bearing stem is manufactured of an extremely hard material, several uses for each set of threads are not significant. The TZM surface, however, shows obvious visual signs of wear after just one use. To verify that the condition of the TZM surface was contributing to the change in strain values recorded, a worn hole was sanded with 60 grit sandpaper. This paper was chosen to produce roughness that was visually comparable to the original machining marks. A torque test showed that the preload partially returned to the preworn level. It was thus determined that new TZM discs should be used to record final measurements. A set of six holes on a TZM disc would be instrumented for each fastener material, so two complete transducers were produced. Each fastener hole would be used four times. The disc used for the I-909 fasteners is shown in Figure 17. Each individual hole would be calibrated individually, so that variations in strain gage placement and orientation, etc, would be accounted for in the calibration.

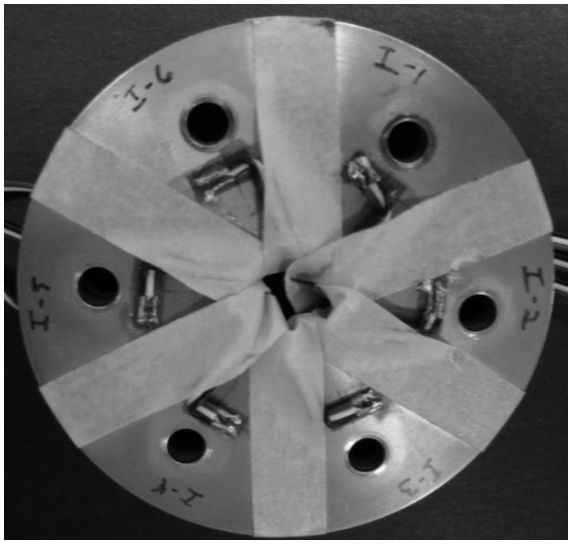

Figure 17: TZM Disc with Strain Gages

Calibration Method and Results

Each individual calibration test resulted in a file containing corresponding load and strain data. The load is plotted on the ordinate and the strain on the abscissa of a chart. The equation of the line is found and used as a calibration equation. A value of strain is simply converted through the equation into the corresponding preload. An example chart with the corresponding equation is shown in Figure 18.

As the tests were performed on four sets of six fasteners, the mean is the average of 24 measurements. The results are listed in Table 2. While the tests were being performed, is was observed that the I-909 tests did not show significant effects of wear, and the A-286 tests showed only small indications, as seen in Figure 19. There was

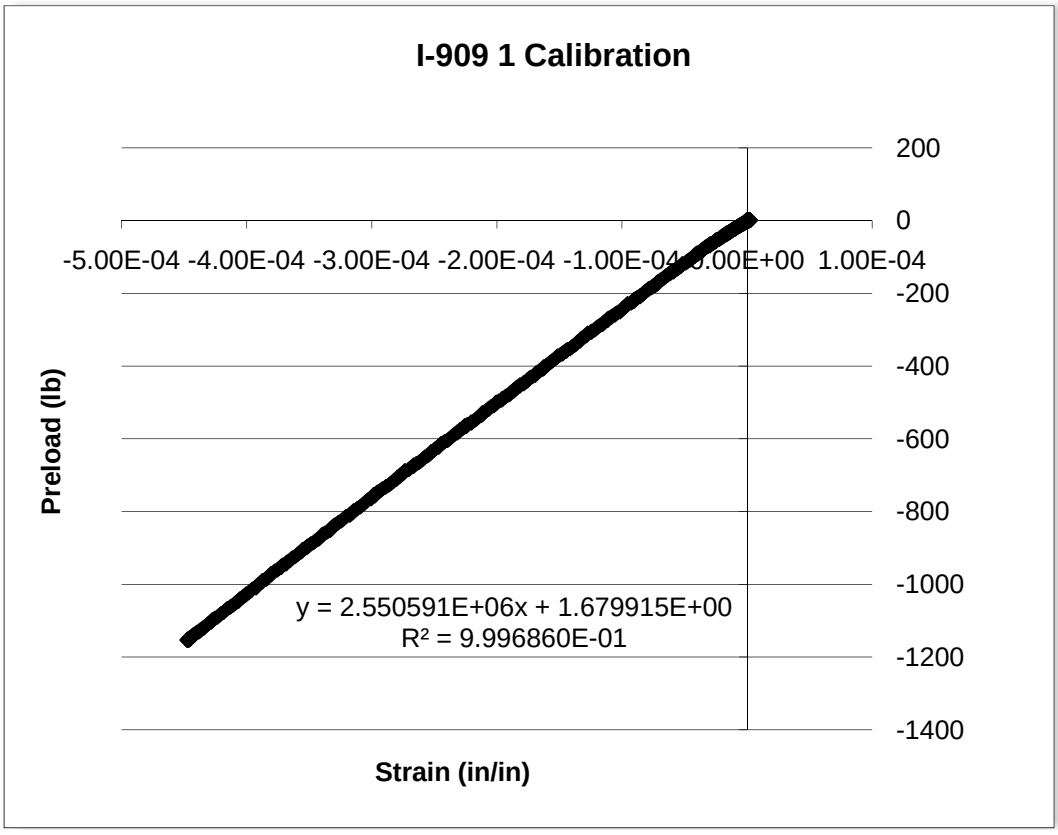

Figure 18: Example Calibration Chart

significant scatter among the six fastener locations in a given set, which is to be expected when controlling preload by torque. It is commonly assumed (7,8) that controlling preload by torque results in ±30-35% accuracy. The I-909 fastener data showed +28 -36% range, and A-286 showed +57 -23% range. The range of A-286 data indicates that the data is skewed toward lower preload values. Variations in the geometry of the components and the surface roughness are some likely causes for scatter. See Figure 20.

Method Applicability

The Joint Strain Calibration Method was developed to solve the problem of measuring the preload in fasteners too small for other methods. This method was developed and utilized for the specific joint of this application, but could be utilized for other joints.

One characteristic of this joint that made the Joint Strain Calibration Method effective was the fact that there is a gap in between the two bodies being clamped. This allows for bending deflection of the bodies and corresponding bending strains. Using this method in a case where there is no gap, and thus no bending strains, would likely results in lower accuracy. The idea of the method, calibrating a response of the joint to preload, could be implemented in a different manner for another application.

Table 2: Final Preload Results

Fastener			Preload
A-286	Mean	lbs	426
	Std Dev	lbs	82
	CoV	%	19.2
I-909	Mean	lbs	696
	Std Dev	lbs	146
	CoV	%	21.0

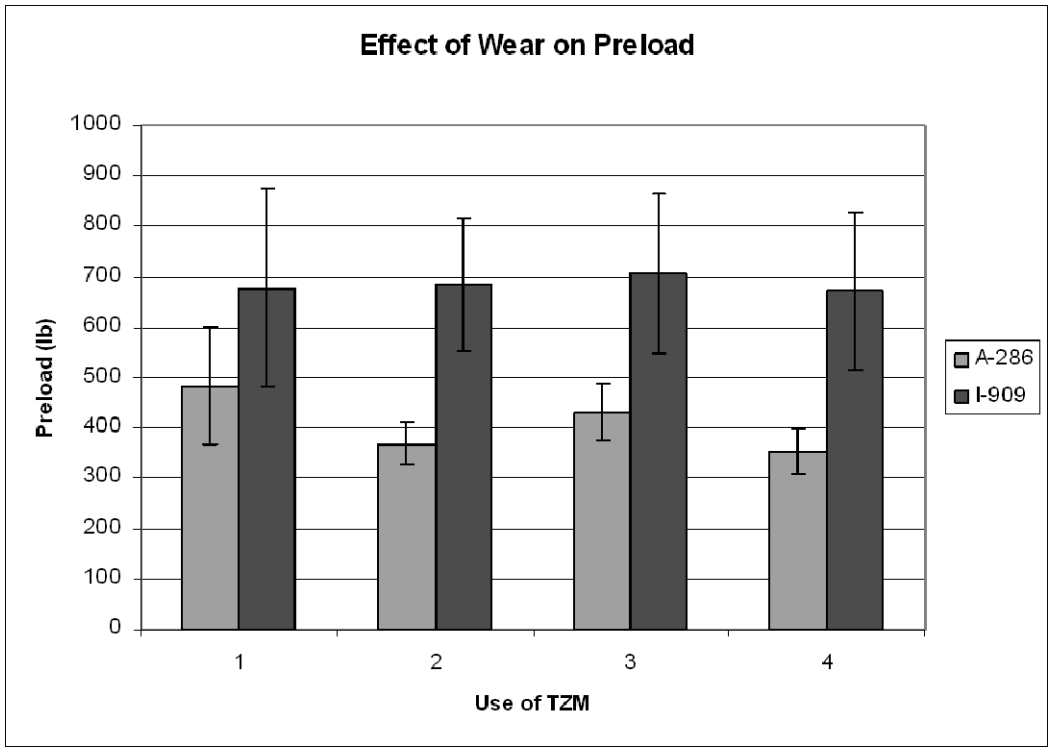

Figure 19: Effect of Wear on Preload

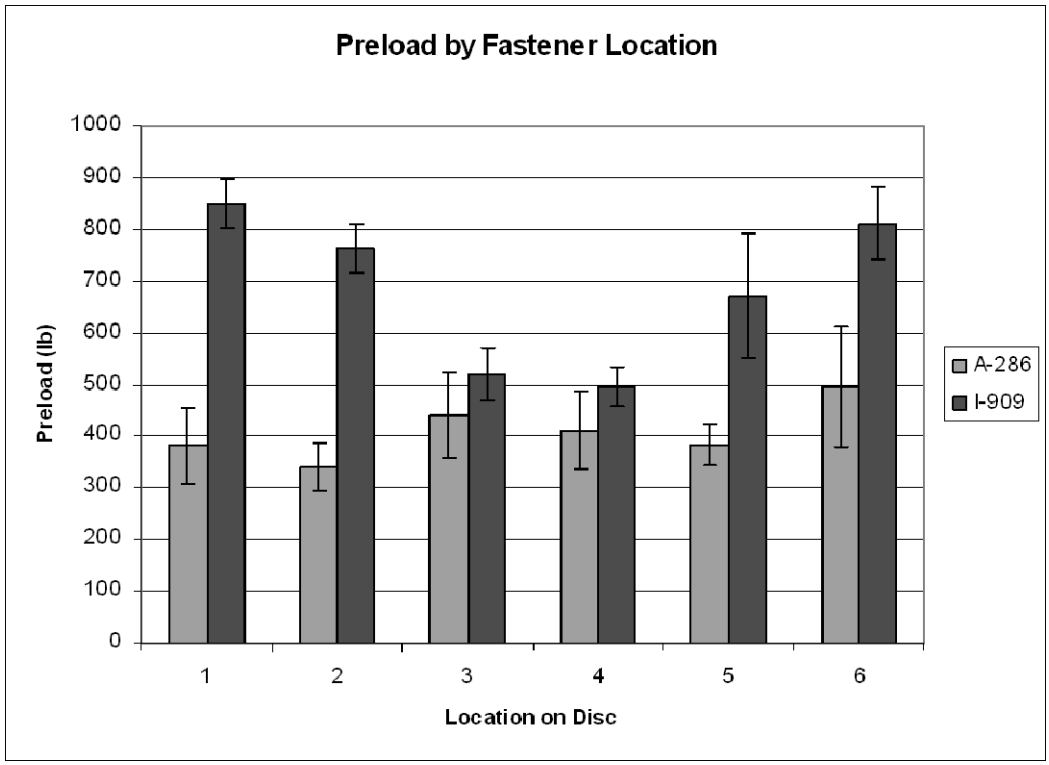

Figure 20: Variation in Preload by Location on TZM Disc

Supporting Calculations

In researching into preload estimation, a NASA document entitled “Criteria for Preloaded Bolts” (7) was indentified. One method it describes for estimating bolt preload is the Experimental Coefficient Method. This method provides an estimation of the maximum and minimum expected preload, having as inputs the fastener dimensions and experimentally determined coefficients of friction between the fastener material and other surfaces. To experimentally determine the coefficients of friction, a simple force balance can be performed on a block resting on plane inclined to the point of slip. Such a block and plane is seen in Figure 21. Note that the mass of the block has been removed from the labels.

In the condition of impending slip, the force of friction is equal in magnitude to the component of gravity acting along the plane, g sinθ. It is also equal to the coefficient of friction times the normal force, which is the perpendicular component of gravity, μg cosθ. It is seen that

$$\mu = \frac{sin\theta}{cos\theta} = tan\theta$$

Equation 10

The coefficient of friction is simply the tangent of the angle at which slip occurs, assuming coulomb friction. A test was set up to increase the angle of inclination of a

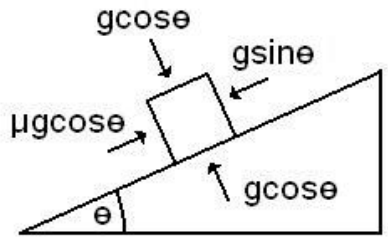

Figure 21: Block on an Inclined Plane

plane to the point of slip, using a vertical stage. A fastener was weighted with a thread die and placed on the surface. The die was used to lower the center of gravity of the fastener so that it would not tip, but slide. At the point of slip, the angle of the plane was measured with a protractor. The test was performed three times for each coefficient needed, and an average value found. Minimum and maximum coefficients of friction are required for each pairing of surfaces. The minimum value occurs with the surface of the plane in a worn state, and the maximum value with an unworn surface. The results are included in Table 3. The test setup is shown in Figure 22.

Table 3: Measured Coefficients of Friction between Surfaces

	TZM New	TZM Worn	WTS New	WTS Worn
A-286	0.238	0.218	0.176	0.155
I-909	0.227	0.217	0.158	0.158

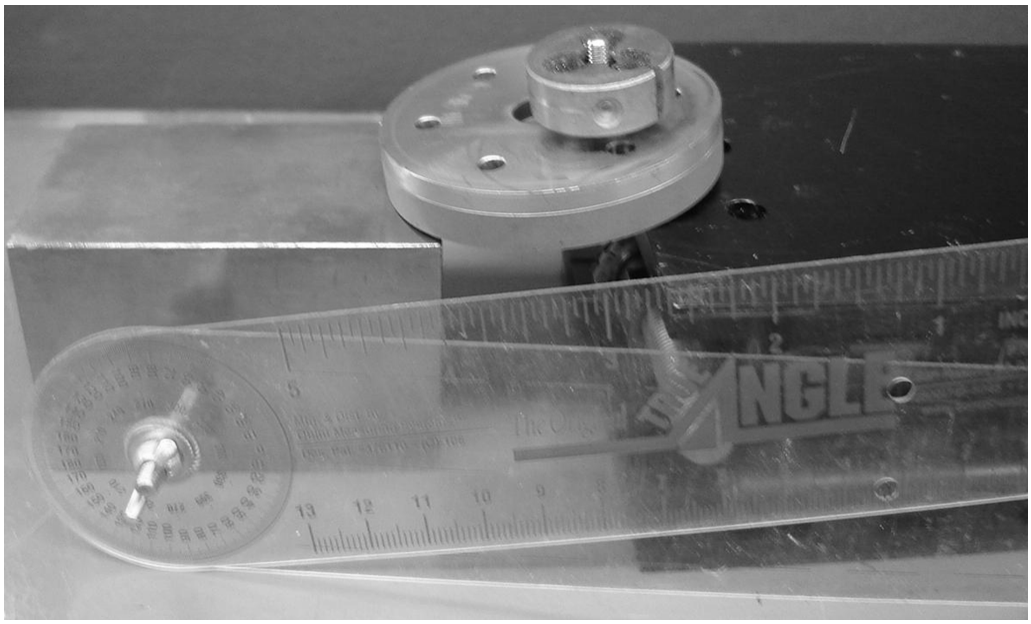

Figure 22: Test Setup for Coefficient of Friction Measurement

The equations for the maximum and minimum preload using the experimental coefficients method are similar to the familiar $T = F_i K d$, and are given as follows:

$$P_{max} = \frac{T_{max}}{\left[R_t\left(tan\alpha + \frac{\mu_t^{min}}{cos\beta}\right) + R_e\mu_b^{min}\right]} + P_{thr}^{pos}$$

Equation 11

$$P_{min} = \frac{T_{min} - T_p}{\left[R_t\left(tan\alpha + \frac{\mu_t^{max}}{cos\beta}\right) + R_e\mu_b^{max}\right]} + P_{thr}^{neg} - P_{loss}$$

Equation 12

P - Preload

T – Applied torque

R_t - Effective radius of thread forces ≈ E/2

E – Basic pitch diameter of external threads

R_e – Effective radius of torqued element-to-joint bearing forces = $(R_o+R_i)/2$

R_o – Outer radius of torqued element

R_i – Inner radius of torqued element

α – Thread lead angle = $\tan^{-1}[1/(n_o \pi E)]$ for unified thread form

n_o – Threads per inch

β – Thread half angle = 30° for unified thread form

μ_t – Coefficient of friction at the external-to-internal thread interface

μ_b – Coefficient of friction at the nut-to-joint bearing interface

P_{thr}^{pos} – Positive thermal load (assumed zero)

P_{thr}^{neg} – Negative thermal load (assumed zero)

P_{loss} – Expected preload loss (estimated at 10% of preload)

The maximum and minimum torque values were assumed to be 41 in-lb (4.63 Nm) and 39 in-lb (4.41 Nm), respectively, because the torque wrench used was marked in 1 in-lb increments. These calculations give a maximum of about 880 lbs (3.91 kN) for both fasteners, and a minimum near 700 lbs (3.11 kN). It should be noted that the common estimate for both coefficients of friction of 0.15 leads to a preload estimate over 1200 lbs (5.33 kN).

A chart (Figure 23) was assembled to compare the maximum and minimum preload values determined for each fastener material. The three methods compared are the proportion utilizing the torque-to-failure data, the NASA equations, and the Joint Strain Calibration Method. The maximum preload calculated by the NASA equations represents the best-case scenario of maximum torque and minimum friction, with no loss. The minimum is the opposite case. The minimum calculated preload depends on the loss assumed, so it is less useful as a bracketing number. The maximum measured preload should correspond to the maximum calculated preload if the test conditions are close to ideal. The cut threads of the I-909 fasteners provide such a condition, but the rough rolled threads of the A-286 fasteners do not. The rough threads would generate larger frictional forces than smooth threads due to larger geometric interferences, resulting in lower preloads with the same coefficients of friction.

Thus, it would be expected that the maximum measured preload for I-909 would agree with the NASA calculated maximum, and the measured A-286 preload would be lower than the calculated preload. The highest measured preload for A-286 was 668 lbs (2.97 kN), which is considerably lower than the calculated upper limit of 880 lbs (3.91

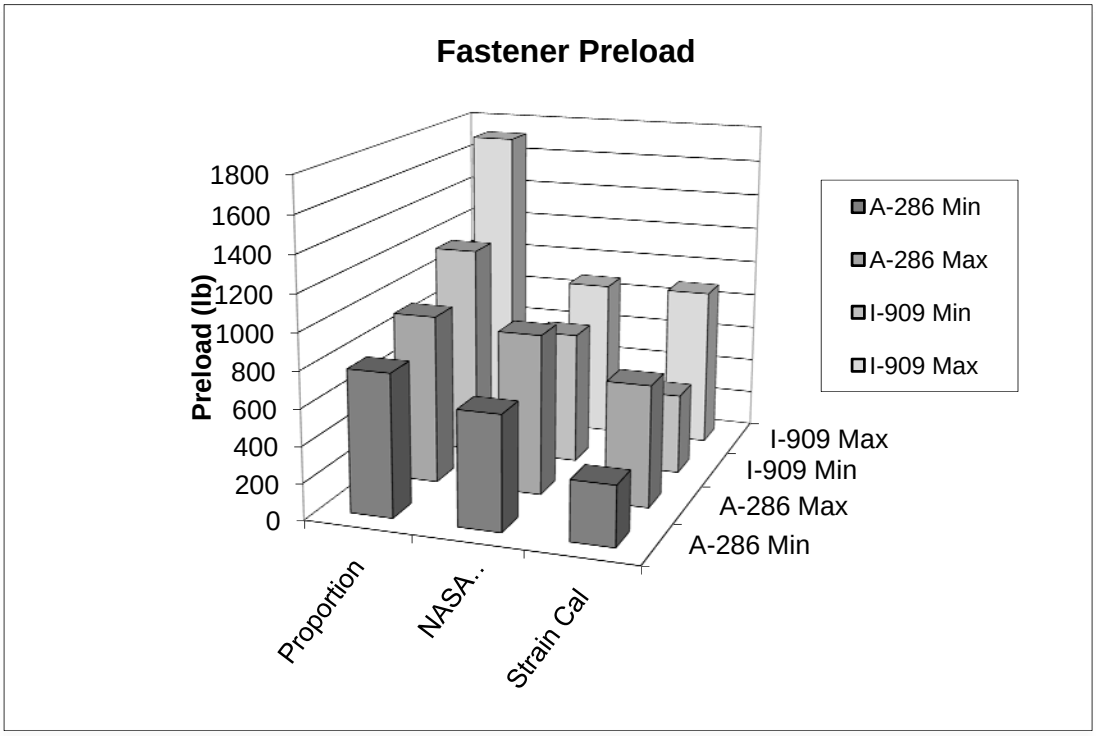

Figure 23: Preload Comparison

kN). The highest measured test value for I-909 was 891 lbs (3.96 kN), nearly within 1% of the NASA calculated value of 880 lbs (3.91 kN). Thus, the NASA equations verify the results of the Joint Strain Calibration Method.

Conclusions

Through research and testing, it was determined that none of the existing preload measurement methods available were well-suited to the small fasteners in this application. A new method, the Joint Strain Calibration Method, was developed that utilizes the existing geometry and materials of the joint to measure the preload. This method could be utilized for other applications, because it involves application-specific calibration. Supporting calculations were performed as well that verify the results.

5: INITIAL FATIGUE TESTING

The purpose of preload determination was to determine the loads needed for the fatigue testing. The alternating load of the fatigue testing is due to the dynamic loading, and the mean load is due to the preload. There two ways of applying the mean load to the fastener. It could be applied by the fatigue testing machine directly, or a fixture could be designed that will load the fastener, and only the alternating load would be applied by the machine. For the initial fatigue testing, the latter method involving a fixture was selected.

Fixture Design

A fixture was designed that would apply the preload by bending of a plate. The lower part of the fixture is a 1 inch (25.4 mm), 14 threads per inch threaded stud with a channel milled into the end of a depth of 0.050 in. (1.3 mm). This milled channel is the same depth as the gap between the surfaces in the actual joint. A hole was drilled at the bottom of the channel and tapped for 8-32 fasteners. The upper part of the fixture is a rectangular prism, one inch square on the bottom and two inches high. A rectangular through-hole is milled through a pair of vertical faces so that ¼ inch (6 mm) wall thickness remains, and the interior corners are rounded. The bottom face is fabricated with only 0.193 inch (4.9 mm) thickness, which is the thickness of the TZM disc. A hole matching the fastener holes in the TZM disc is made in the center of this lower face, and the upper face includes a larger threaded hole to attach to the upper portion of the testing

machine by another threaded stud. The fixture is shown in Figure 24. As the fastener is preloaded, the bottom face of the prism deflects into the recessed area. This design permits a strain gage to be placed on the bottom surface of the prism and calibrated, so it would be known when the proper preload was applied.

The fixture was calibrated by mounting it into the 3.3 kip testing machine and recording the strain of the gage at 100 lb (445 N) intervals. The relationship between load and strain was linear. To preload a fastener, it was tightened until the strain corresponding to the desired preload was indicated. Figure 25 shows the 3.3 kip testing machine.

Figure 24: Preloading Test Fixture

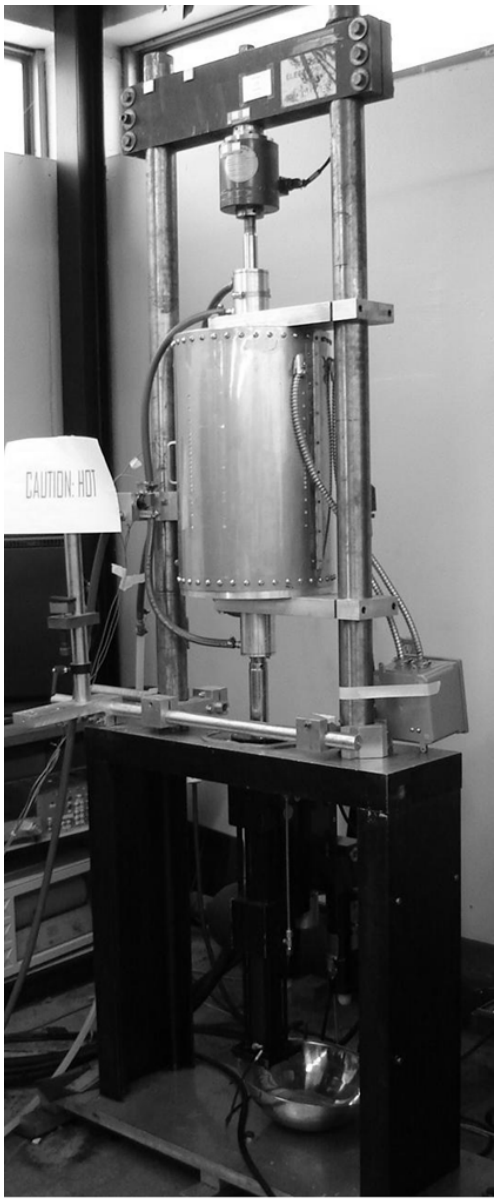

Figure 25: 3.3 Kip Servo-Hydraulic Testing Machine

Initial Room Temperature Testing

The test program for this fatigue testing was relatively simple. The test was to be a load-controlled sinusoid that would continue until failure. The load bounds were discussed previously in Chapter 3. The test program began with a ramp to the lower load bound, at which point cycling began between the minimum and maximum load at the specified frequency. The frequency of cycling was 40 Hz for the first test, and was 50 Hz

for subsequent tests. This would continue until the test was stopped manually or a load or displacement limit was tripped. Failure of a fastener would result in at least one limit being tripped. As linear data acquisition is impractical for fatigue testing, logarithmic data acquisition was used. Five cycles (successive peaks and valleys in the load) were recorded every time the leading number on the cycle count changed. This method of data acquisition results in data by ones to ten, by tens to 100, by 100s to 1000, etc.

The first test performed was an I-909 fastener at room temperature. The test ran for 21 days at 40 Hz, or over 72 million cycles. It was only stopped then because of a cable connection issue. The fastener showed no obvious visual signs of cracking or wear. Due to the extremely long nature of this test, it was decided that there needed to be a criterion to stop a test that is essentially an "infinite life" test. A simple criterion would be reaching without failure a multiple of the cycles to failure of tests that do fail. As failures were observed in A-286 fasteners in service at high temperatures, it was decided that high-temperature A-286 tests should be performed first. If other specimens do not fail within a decided multiple of the average lifetime of the high temperature A-286 tests, the tests could be stopped as 'no failure' or, to use a more common term, a runout.

Initial High Temperature Testing

To perform the high temperature tests an environmental chamber had to be set up on the testing machine to maintain high temperatures. The hydraulic actuator and load cell had to be kept cool to prevent damage. It was advantageous that the testing did not need to be performed in a vacuum, as that would have necessitated heating by radiation alone, which is much more difficult than heating by convection.

The 3.3 kip test machine has been used for fatigue testing in the past, so existing hardware for previous test programs proved useful. A large oven was utilized that was designed to fit onto the 3.3 kip load frame, and it appeared to have a high temperature capacity. It is a cylindrical clamshell unit, about 21 in. (530 mm) long, opening into two halves along its 13 in. (330 mm) diameter. The heating elements are encased in ceramic cylindrical shells, with 4 in. (100 mm) of insulation between the heating elements and the metallic outer shell. The end caps are aluminum, and to the caps are attached mounting arms that clamp to a post of the load frame. There are several holes in vertical lines on the sides of the unit for insertion of temperature sensors. The control unit used with the oven was utilized as well. The equipment was functional and able to obtain temperatures up to 750 ºF (400˚ C). Minor repairs were required for the insulation. The oven in its original condition is shown in Figure 26, and after repairs in Figure 27. In a dry run, the controller managed to heat the oven up to 750 ºF (400˚ C) with little overshoot, and held the there to within a few degrees. It appeared that the original tuning of the controller was well suited for this application; therefore no settings in the controller were changed.

Water jackets that were designed to fit over the hardware of the 3.3 kip machine were also utilized. They are cylinders made of aluminum, 3 in. (75 mm) diameter and 4 in. (100 mm) long. The 1 in. rods that connect to the actuator and load cell fit through an axial hole. The water jackets are actually C-shaped, with a very small gap. The water enters and exits through brass fittings, mounted on the outer wall on either side of the gap, at opposite longitudinal ends. The jackets were tested to assure that they did not leak. They appeared to have no problems and require no repairs. A mounted water jacket is pictured in Figure 28.

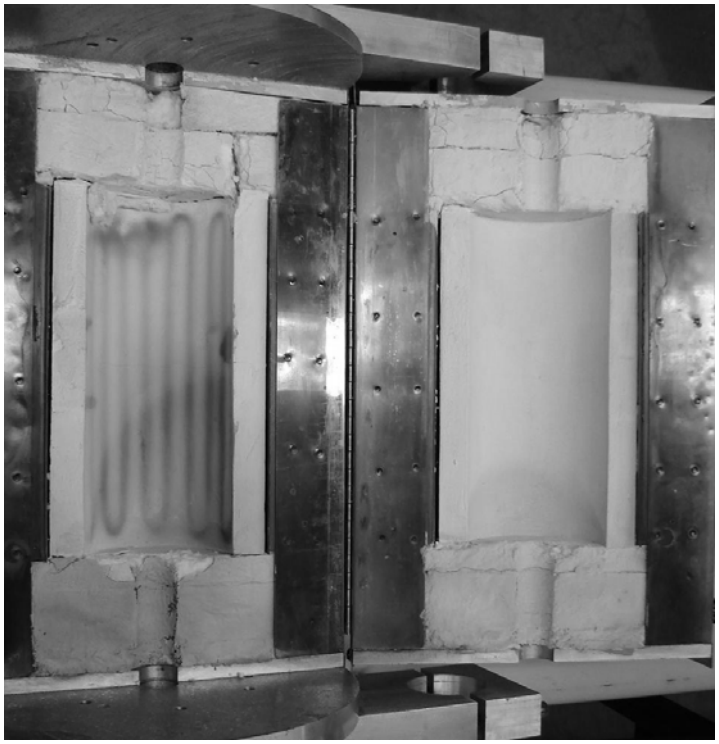

Figure 26: Oven before Refurbishment

Figure 27: Oven after Refurbishment

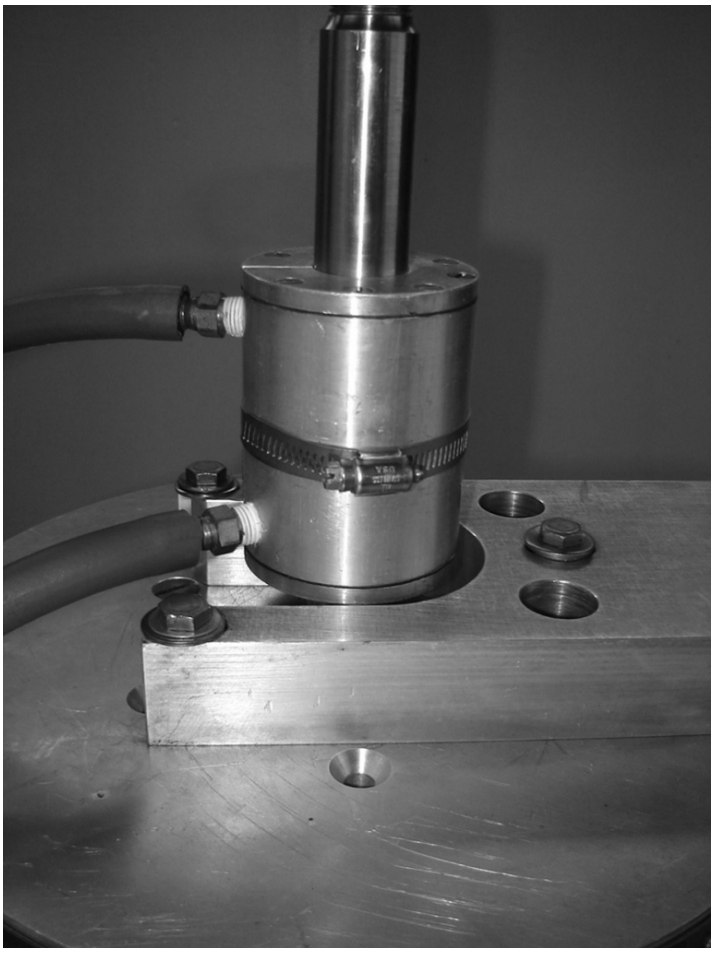

Figure 28: Water Jacket above Oven

The oven was mounted onto the load frame and wired to the controller. The water jackets were mounted as well, one above and one below the oven, as shown in Figure 29. Water was brought in from a nearby water line through a hose that branches to each jacket, and the outlets join together and are run down a drain pipe.

The load conditions for the high temperature tests had to be determined. In a meeting with the customer, it was decided to use the room temperature preload, and then replicate the thermal expansion that occurs in the actual joint. The thermal expansion characteristics were replicated so that the preload would change the same way as it does in service. In accordance with this decision, a new fixture was made, just like the

Figure 29: Oven and Water Jackets Mounted on Machine

previous one, but with the prism constructed of TZM instead of steel. The new fixture was gaged and calibrated as the previous one, but because the strain gages would not survive 750 ºF (400 ˚C) it was decided to control the preload by torque after the calibration.

The fixture was attached to the 3.3 kip test machine and loaded using a calibration test that was written specifically for this fixture. The test was simply a load ramp that stopped for 30 seconds every 100 lbs. (445 N) from 100 to 1000 lbs (4.45 kN). The

pause was to take strain readings after the load stabilized at each interval. From these readings, it could be determined what value of strain corresponds to a given preload and specifically, what values of strain correspond to the preload determined for the two different fasteners. The chart of the readings is included in Figure 30.

The next step was to obtain data relating strain and torque. As it has been seen previously that TZM exhibits wear quickly, it was desired to obtain a uniform state of wear that would not further change. As a result, the calibration would not have to be redone for each specimen, which would be time consuming and require the application of a strain gage to the fixture for each specimen. It was desired to simply determine the value of torque for this fixture that would produce the same strain that was seen at the predetermined preload value for each material.

For a torque value to be determined, the strain readings at 40 in-lbs (4.5 Nm) of torque would need to stabilize after several uses. The strain reading dropped significantly in the first few uses (down 60% in the first three) and continued to drop slowly. It was noted that if an hour were let pass between tests, the strain readings would be higher than the previous test. One possible cause was that an oxidation process was potentially occurring at the surface and was being abrasively removed by the fastener head. Whether or not an oxidation process was the cause, the strain developed by a given torque depended on wear and time.

It was also seen that the strain readings never returned to the original maximum value, but would increase up to a certain amount after 24 hours. This value was used as the baseline, as the variability seemed to stabilize. The corresponding torque values were determined to be 47 in-lbs (5.3 Nm) for A-286 and 51 in-lbs (5.8 Nm) for I-909. The

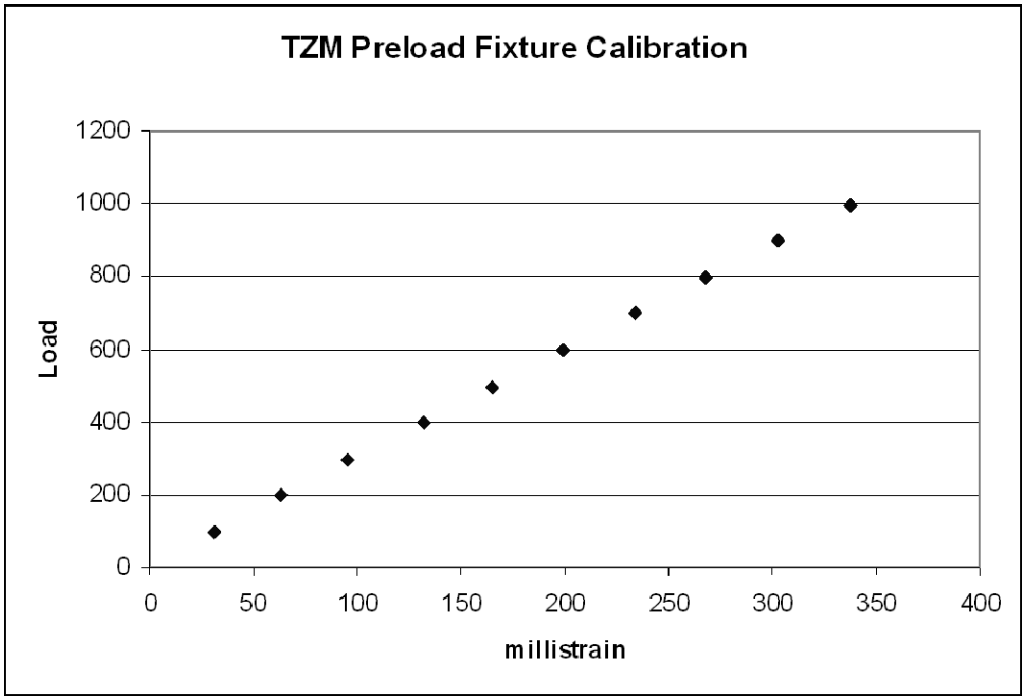

Figure 30: TZM Preload Fixture Calibration Data

values were obtained by scaling based on the strain desired for the given fastener, and the strain obtained from a 40 in-lb (4.5 Nm) test after a wait of 24 hours.

Results of Initial Tests

Two tests were performed on A-286 fasteners, and both went over 50 million cycles before they were stopped for extraneous reasons. It seemed that the physical mechanism that caused the failure in the fasteners in service was not being replicated. As previous work on thermal expansion of the bolted connection had shown that the bolt preload could be going to zero near 750 ºF (400˚ C), it was suspected that impacting and vibration due to a loose joint rotating at 110 Hz could be an important factor in causing fatigue damage. This type of loading is not replicated by servo-hydraulic testing. To determine if joint instability was a potential issue, it was decided to do a detailed finite element model of the preload in the joint over a wide temperature range.

6: FINITE ELEMENT ANALYSIS OF TEMPERATURE EFFECTS ON PRELOAD

The purpose of the finite element analysis was to determine the effect of temperature on the preload in this particular bolted joint. The basic approach was to model the joint in Solidworks, import it into ANSYS, apply the preload, and then subsequently vary the temperature.

Solid Model

The TZM disc, a portion of the bearing stem and a fastener were modeled in Solidworks. A version of each part was made to correspond to a 1/12 model of the joint, a wedge from the center of one hole midway to the next one. This required a 30˚ wedge of the TZM disc and bearing stem, and one half of a fastener. The fastener was modeled as a single volume with the bearing stem to avoid surface contact problems at the "threads." It was assumed that the threads prevent any fastener motion relative to the bearing stem, especially because the actual fasteners in the actual application are secured to prevent rotation and unthreading. The bearing stem and fastener were made into separate volumes after being imported into ANSYS. The TZM disc was modeled as a separate volume because it needed to have freedom to move relative to the other pieces. The two volumes were put together in an assembly, and saved as an IGES file to be imported into ANSYS.

ANSYS Script File

A script was written in ANSYS that would perform all of the analysis. It first imported the IGES file, and then created the three volumes: the disc, the fastener, and the bearing stem. It was at this point that the fastener was created as a separate volume from the bearing stem, but still shared boundary lines and surfaces. This process assured that the mesh would match up exactly inside the fastener hole. If the mesh did not match exactly, there could be penetration problems and the model would not function properly. The mesh was generated manually to obtain proper refinement near the fastener. The mesh is shown in Figure 31.

Material properties were assigned to each volume. Standard surface contact pairs were created between all interacting surfaces (except in the "threaded" portion of the fastener hole, where they are not necessary). A pretension element was then created in

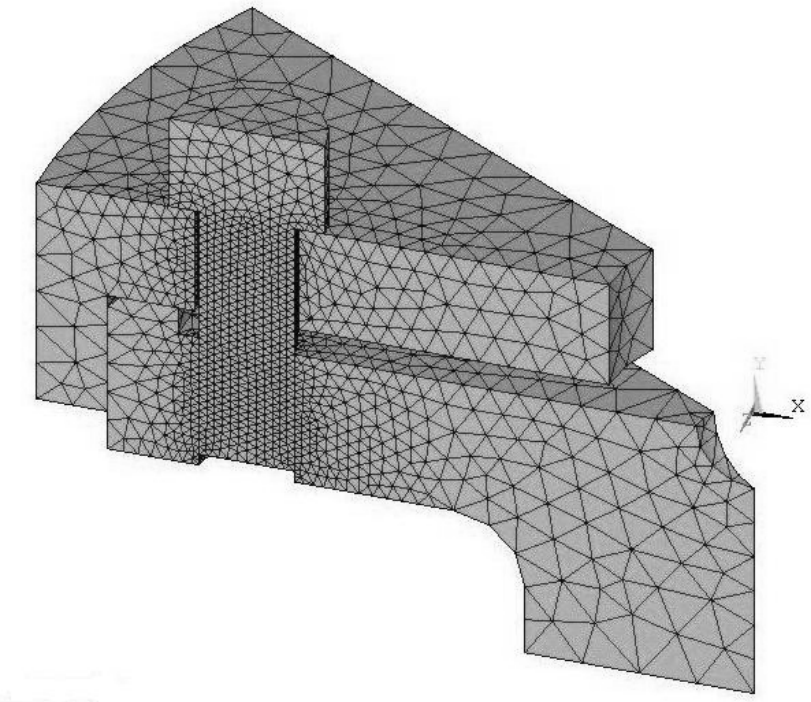

Figure 31: Finite Element Mesh for Preload Model

the fastener, which is a built-in element in ANSYS used specifically for the preloading of fasteners. It assures that the resultant force of the stresses in the cross section of the fastener is equal to the set value. The model was then constrained and solved, so that the stresses in the joint due to preload could be seen. The model was then restarted and a new uniform temperature was applied. The resultant force across the pretension section can be read after resolving, which indicates the change in preload due to thermal expansion. A Y-direction stress plot (axial in the fastener) of an I-909 fastener at 750º F is shown in Figure 32.

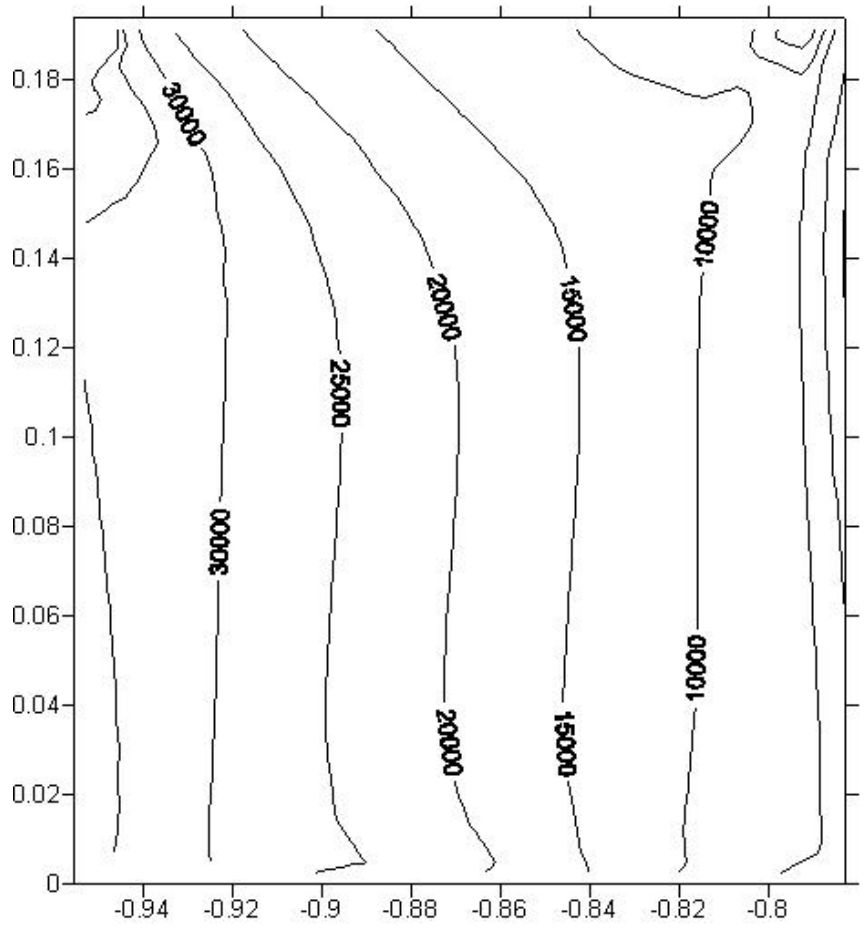

Figure 32: Axial Stress in I-909 Fastener at 750 ºF

Results of Finite Element Analysis

The preload was determined at every 75 ˚F (42 ºC) from 0˚ (-18 ºC) to 825 ˚F (441 ºC), so that the relationship could be seen. A preload of 800 lbs (3.56 kN), or 400 lbs (1.78 kN) on the half-fastener, was used for the I-909 model and 500 lbs (2.22 kN), or 250 lbs (1.11 kN) on the half-fastener, for the A-286. It was seen that the preload of the I-909 increased to a maximum near 225 ˚F (107 ºC), and then decreased through 825 ˚F (441 ºC), as shown in Figure 33. The overall range was very small, however, and at the 750 ˚F (400 ºC) fatigue test temperature, the model estimates that the preload is still over 750 lbs (3.34 kN). The A-286 model showed an almost linear decrease in preload until it reached a no-load condition around 450 ˚F (232 ºC), and remained unloaded at temperatures beyond.

Because the preload in the A-286 fastener goes to zero at 450 ˚F (232 ºC), preload is no longer a good measure of the condition of the joint. Consequently, the gap

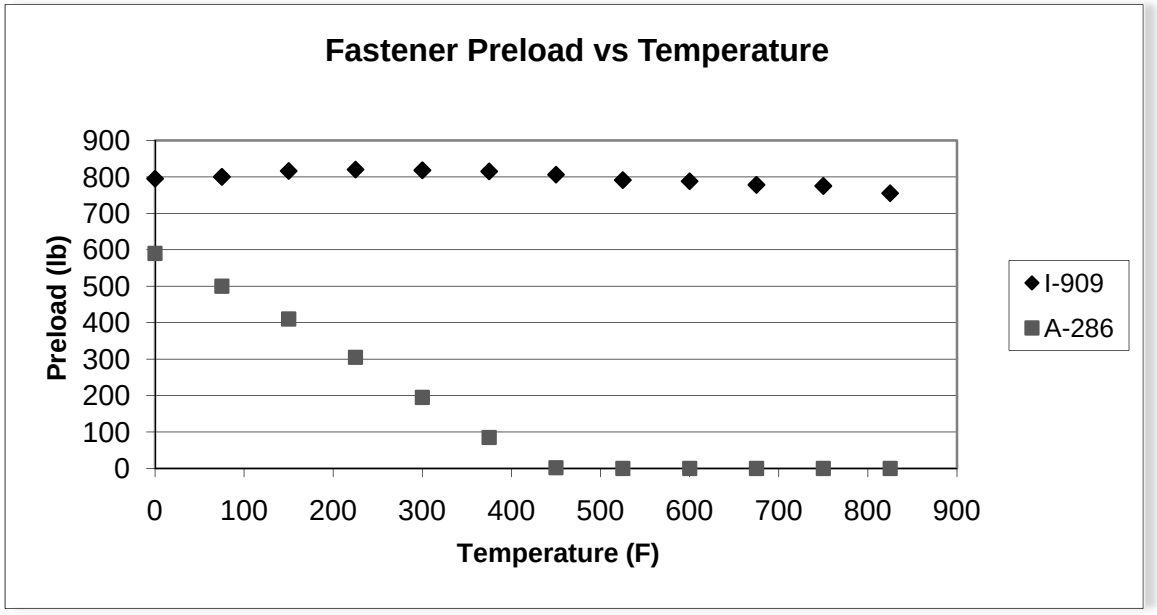

Figure 33: ANSYS Model of Preload vs. Temperature

between the underside of the fastener head and the TZM disc was determined. The gap is essentially zero up to the 450 ˚F (232 ºC) point, and after that it increases linearly to 0.0005" (12.7 μm) at 825 ˚F (232 ºC). It is non-zero while the surfaces are in full contact because the locations are determined by gauss points, and not the corner nodes. A chart of the modeled gap is shown in Figure 34.

The finite element analysis results suggest that the I-909 fasteners are not losing significant preload due to thermal expansion, and therefore the joint remains stable. The A-286 fasteners can and probably do allow relative motion between the TZM disc and the bearing stem at temperatures above 450 °F (232 ºC). This would lead to vibration in a joint that is rotating at 110 Hz, and this vibration and related impacting are a possible explanation for the fatigue failures observed with the A-286 fasteners. It is noted that the mechanical testing performed for this project does not replicate the effects of looseness or impacting. Consequently, a new approach was taken with the fatigue testing to be done.

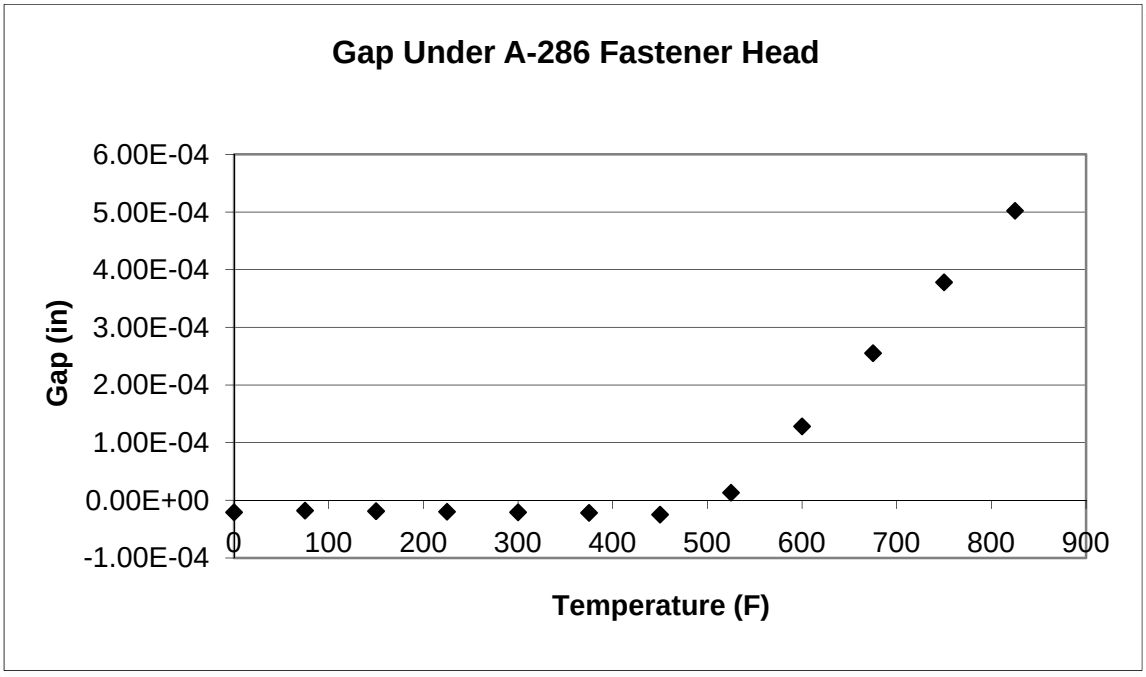

Figure 34: Gap under A-286 Fastener Head

Based on results from finite element analysis, it was decided that instead of determining the life of the fasteners at the in-service load levels, life-load data would be generated at several different load levels. This data could be used to estimate the life of the fasteners. It is also suspected that the in-service fatigue failures that occurred with A-286 fasteners were not due solely to the dynamic loading, but also to the instability of the joint at high temperature. Data at higher load levels than the in-service conditions, but with longer life, could be used to investigate this further.

7: FINAL FATIGUE TESTING

As discussed previously, the previous fatigue tests were not at loads of sufficient magnitude to produce fatigue failures in a reasonable amount of time. It was decided that the fatigue load levels should be chosen as percentages of the ultimate load for each fastener at each test temperature. Consequently, tensile tests were required to determine the ultimate strength of each material at each temperature. These tests were performed on the 3.3 kip test machine with a modification of the spring constant test fixture.

Tensile Strength Testing

The fixture used for the tensile tests was a combination of previous fixtures. The upper fixture component designed for the spring constant testing was of 0.5 in. (12.7 mm) diameter. There are studs that connect to the 3.3 kip test machine that have a 0.5 in. threaded hole, so the outer surface of the fixture was threaded so that it would simply screw into one of the studs. The lower half of the original fatigue fixture could still be used, and the milled channel became unimportant.

Tensile tests were performed on three specimens for each material at each of three temperatures: 750, 480, and 72 °F. The tests were performed with a constant displacement rate of 0.0175 in/min (4.445 mm/min). There was very little scatter and the failure of each fastener of a given material appeared the same. The A-286 fasteners failed on an inclined plane across three or four threads. The I-909 fasteners failed on a smooth section at 90° to the loading direction. The failure always followed the root of a

thread around for an entire revolution. This failure mode may be due to a combination of less ductile behavior and the large stress concentration at the root of the cut threads. The results of the tensile tests are included in Table 4.

The A-286 fasteners showed a moderate decrease in ultimate load with temperature, and the I-909 fasteners showed only a slight decrease. The two higher temperatures resulted in almost identical ultimate loads for I-909. Comparing 750° F (400 ºC) with 72 ºF (22 °C), it is observed that 88% of the ultimate strength of A-286 remains, and the ultimate strength of I-909 is still nearly 97% of its room temperature value.

Fatigue Testing

The same fixture that was used for tensile testing was used for fatigue testing. Initially, high temperature tests were performed as it was expected that they might be shorter in duration than tests at the same percentage of ultimate load at lower temperatures. The first tests would be performed to determine which percentages of ultimate load would be used for the final tests. After the percentages were determined, testing went forward with three specimens being tested at each temperature for each material. Room temperature and 750 ºF (400° C) would be performed first, as it was

Table 4: Ultimate Load Results from Tensile Testing

			72 F	480 F	750 F
A-286	Mean	lbs	2772	2601	2439
	Std Dev	lbs	64	44	51
	CoV	%	2.3	1.7	2.1
I-909	Mean	lbs	2261	2186	2188
	Std Dev	lbs	59	103	45
	CoV	%	2.6	4.7	2.0

possible that the intermediate temperature of 480 º F (250 °C) might be unnecessary due to lack of temperature effects. The percentages chosen were 60, 50, 40, 30, and 20%.

A criterion was needed to stop tests that were running too long. The fatigue failures that occurred in the bolted connections of the original application occurred at or before about one million gantry rotations. Using the gantry rotation speed and the bearing rotation speed, it was determined that one million gantry rotations corresponds to 39 million bearing rotations or fatigue cycles. At the 50 Hz testing speed, 39 million cycles takes about 9 days. 40 million cycles was deemed an acceptable stopping criterion by the client. Once a specimen was stopped without failure at 40 million cycles, additional specimens at that load and temperature were not tested.

Testing Results and Temperature Effects

Because all of the fatigue testing was done with the same R value (R = 0.1814), each individual test is adequately described by its maximum load. The cycles to failure of the tests are presented in Table 5, listed with the maximum load. It is noted that there was never a failure between 500,000 cycles and complete runout at 40 million cycles. It can also be seen that the A-286 fasteners outperform the I-909 fasteners at 60, 50 and 40 % of ultimate load. As the loads get lower, the results for the two typed of fasteners converge. Three of the four tests over 40 million occurred in the 20 % range. The exception was A-286 at 750 º F (400ºC), where runout occurred at 30%. It is thought that this may be due to the material becoming more ductile at high temperature, and thus resisting fracture for a longer period.

The effect of temperature is more clearly seen in Figure 35 and Figure 36, which

Table 5: Fatigue Testing Results

	A-286				I-909			
	25 C		400 C		25 C		400 C	
%	Load	Cycles	Load	Cycles	Load	Cycles	Load	Cycles
60	1662	24154 19890 26650	1464	13551 13073 20794	1356	2595	1314	3825
50	1385	29804 24016 28712	1220	25780 24652 25361	1130	5950 6655 4245	1095	6697 4372 4498
40	1108	52482 39869 54630	976	57283 56864 43701	904	25095 6035 21399	876	11695 9739 21593
30	832	56792 101585 162310	732	80980 84172 53000000	678	91533 96588 128231	656	47027 33174 106331
20	554	261801 42835408	488		452	324841 40000000	437	33058634

are semi-log plots. There is no pronounced effect due to temperature other than the fact that the A-286 data levels off at a higher load. Due to the lack of temperature effects, the testing at 480º F (250º C) was not performed. Temperature independence was suggested to be contingent on the absence of environment or sufficiently high frequency of cycling. The fact that the tests were temperature independent confirms that testing in air at sufficient frequencies can be equivalent to testing in a vacuum.

It is seen that even at high temperature, maximum loads over 400 lbs (1.78 kN) can run the equivalent of one million gantry cycles. The maximum load in service is only 140 lbs (623 N). This result suggests that the failures that occurred in service were not solely caused by fatigue due to the dynamic loading alone. Further, the results of this investigation suggest that the instability in the joint due to thermal expansion that may have contributed to the failures of the A-286 fasteners. These results also explain why I-909 fasteners have not been failing in service.

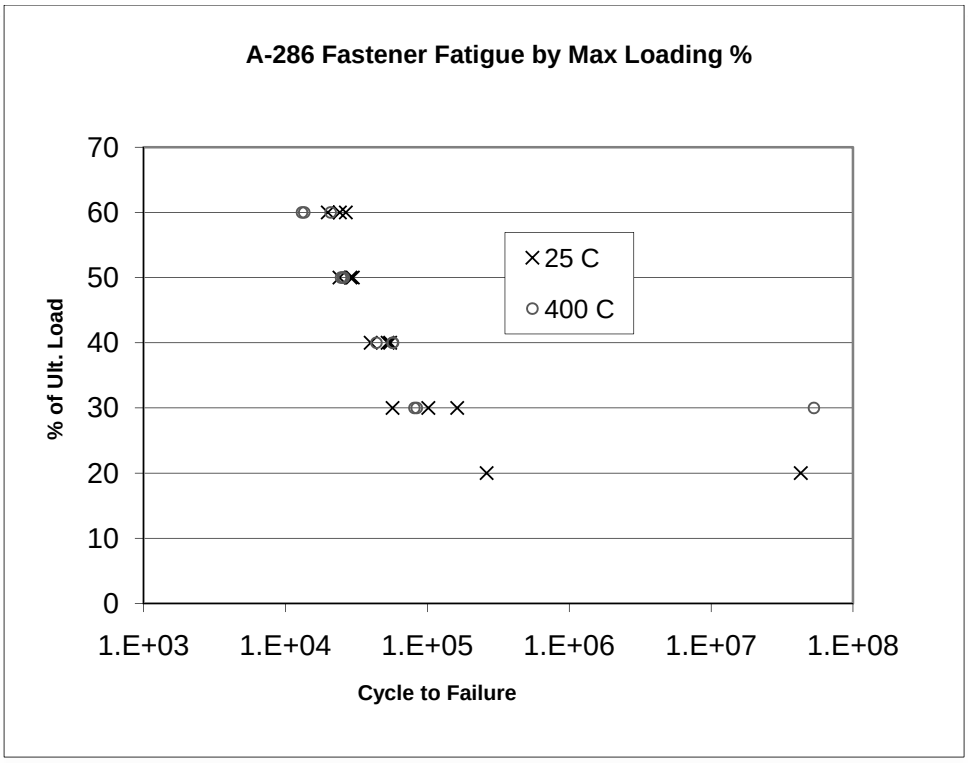

Figure 35: A-286 Fatigue Testing Results

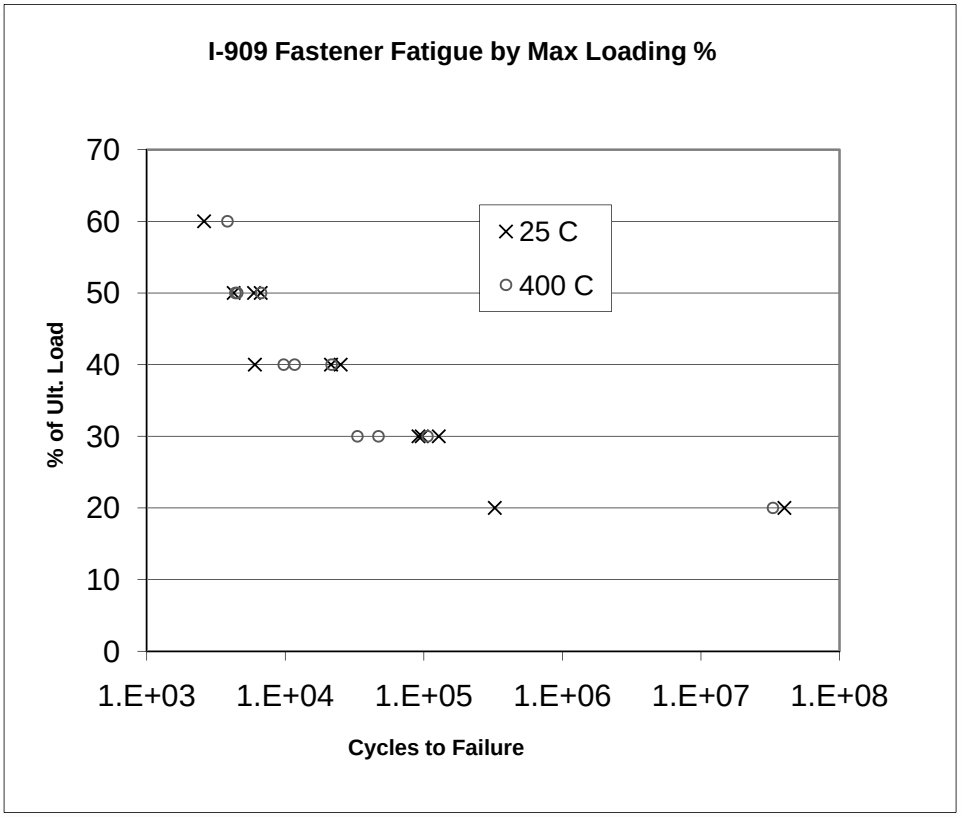

Figure 36: I-909 Fatigue Testing Results

8: CONCLUSIONS

Many of the conclusions reached during the course of this project have been discussed previously in this document. The key points will be highlighted here for emphasis.

Preload Determination/Behavior

After investigating several different methods, a new method was developed that utilized the existing joint as a transducer to measure the preload. The Joint Strain Calibration Method requires the addition of strain gages to the joint and calibration using a testing machine. This method can be utilized with fasteners that are too small for other commercially available methods. It also does not rely on many of the assumptions used in other methods. It only relies on the accuracy and precision of the calibration.

This method was utilized to measure the preload of the fasteners. The preload was determined to be about 700 lbs (3.11 kN) for the I-909 fasteners and about 425 lbs (1.89 kN) for the A-286 fasteners. These preload test results are considerably less than were expected based on equations with estimated parameters.

Finite Element Model

A finite element model was developed in connection with the Joint Strain Calibration Method, but more important was the model of the effects of preload on temperature. Results showed that a 500 lb (2.22 kN) preload in an A-286 fastener goes to zero well below the estimated temperature of the joint in service. At 750º F (400 ºC), it is

predicted that there is a gap under the fastener head. The I-909 fasteners only lose about 50 lbs. (222 N) of an initial 800 lb (3.56 kN) preload. This fact suggests that the maintenance of preload prevents the I-909 fasteners from failing.

Testing Approach

The approach for fatigue testing was originally intended to determine the life at the actual loading conditions. After it became clear that the tests were going to be of extremely long duration, it was decided to determine the life at various load levels and temperatures. This would be done at lower and lower load levels until a sufficient portion of the fatigue curve was obtained. Tests were stopped when after 40 million cycles, the point at which all of the failures had occurred in the actual application.

Fatigue Results

The approach of testing at multiple load levels resulted in data that followed the usual pattern for fatigue data: the data leveled off as loads decreased. The load of runout tests was still at least three times the load actually seen in service. This supports the conclusion that the fatigue failures that occurred were not due to pure fatigue from dynamic loading. This data was independent of temperature, so testing at the intermediate temperature was not performed. Temperature independence was suggested by some of the literature, and it was confirmed to be the case at this high frequency of testing.

Cause of Failure

Results obtained in this investigation suggest that the fatigue failures of the A-286 fasteners were due to an increase in load from impact loading and/or vibration.

Impacting and vibration were in turn caused by looseness and instability in the joint due to thermal expansion in the fasteners. Thus, fasteners with a lower thermal expansion coefficient maintain preload and thus stability in the joint.

Design Methodology

Results of this investigation suggest that proper design will have to include many considerations regarding fastener preload. For future joints with higher rotational speeds and loading, proper joint design will be essential to safe operation. Recommendations for the design of future joints are given below.

The modeling and testing of the preload of a joint must be considered as an important step in the joint design. A common engineering text recommends that a removable fastener should be tightened to 75% of its proof strength for optimum performance in static and fatigue loading.(8) The preloads currently being attained are much lower than this. It is recommended that the target preload be a higher percentage of the proof strength of the fastener.

Using the Joint Strain Calibration Method to measure preload will allow better measurement of the preloads being attained. It is important to know what level of preload is being attained for further analysis, whatever the method used.

This work shows that it is essential to understand the behavior of preload over the range of operating temperatures. It is recommended that a finite element model similar to that performed in this study be utilized for any joint that is safety critical. It is essential that sufficient preload remain to maintain stability in the joint.

Any design with higher target loads will require an increase in fastener size. There is a considerable safety margin in the current design as determined by the fatigue

testing of this study. Increasing the load will lower the safety margin, and thus larger fasteners will be required.

New testing must be performed for any new design. The data generated in this study only applies to the components and load conditions tested. Based on the experience gained during testing, some recommendations on future testing can be made:

- Preload (mean load) should be applied directly by the testing machine and not by a fixture or by a method such as the Goodman relation. This method removes the calibration and repeatability problems of a fixture and the inaccuracies of mean stress relations.
- Testing should be performed in room-temperature air with a frequency of at least 40 Hz. Future testing (on the same materials) will not require testing at multiple temperatures.
- Because the testing would not be performed on multiple materials at multiple temperatures, the test cutoff should be increased. A cutoff of 100 million cycles or higher would be much better.
- More specimens should be tested (at least 6) to allow the use of statistics and confidence estimation.

APPENDIX A

ANSYS CODE FOR TZM DISC MODEL

```
! Elements and Properties
/prep7
et,1,45
mp,ex,1,45e6
mp,prxy,1,.3764
csys,1

! Geometry
k,1,.25,90
k,2,.25,30
k,3,.25,-30
k,4,.25,-90
k,5,.6,60
k,6,.6,0
k,7,.6,-60
k,8,.95,70
k,9,.95,50
k,10,.95,10
k,11,.95,-10
k,12,.95,-50
k,13,.95,-70
k,14,1.126,90
k,15,1.126,75
k,16,1.126,60
k,17,1.126,45
k,18,1.126,30
k,19,1.126,15
k,20,1.126,0
k,21,1.126,-15
k,22,1.126,-30
k,23,1.126,-45
k,24,1.126,-60
k,25,1.126,-75
k,26,1.126,-90
k,27,1.209,90
k,28,1.209,75
k,29,1.209,60
k,30,1.209,45
k,31,1.209,30
k,32,1.209,15
k,33,1.209,0
k,34,1.209,-15
k,35,1.209,-30
k,36,1.209,-45
k,37,1.209,-60
k,38,1.209,-75
k,39,1.209,-90
local,11,1,0,.966
k,40,.094,90
k,41,.094,0
k,42,.094,-90
k,43,.125,90
k,44,.125,0
k,45,.125,-90
local,12,1,.837,.483,0,-60
k,46,.094,0
k,47,.094,90
k,48,.094,180
k,49,.094,-90
local,13,1,.837,-.483,0,-120
k,50,.094,0
k,51,.094,90
k,52,.094,180
k,53,.094,-90
local,14,1,0,-.966
k,54,.094,-90
k,55,.094,0
k,56,.094,90
csys,1
L,1,2
L,2,3
L,3,4
L,1,45
L,45,42
L,1,5
L,2,5
L,2,49
L,2,6
L,3,6
L,3,53
L,3,7
L,4,7
L,4,56
L,5,45
L,5,8
L,5,9
L,5,49
L,6,49
L,6,10
L,6,11
L,6,53
L,7,53
L,7,12
L,7,13
L,7,56
L,41,44
L,44,8
L,9,48
L,46,10
L,11,52
L,50,12
L,13,55
L,40,43
L,43,14
L,44,15
```

```
L,8,16
L,16,9
L,17,48
L,47,18
L,46,19
L,10,20
L,20,11
L,21,52
L,51,22
L,50,23
L,12,24
L,24,13
L,25,55
L,54,26
L,14,15
L,15,16
L,16,17
L,17,18
L,18,19
L,19,20
L,20,21
L,21,22
L,22,23
L,23,24
L,24,25
L,25,26
L,14,27
L,15,28
L,16,29
L,17,30
L,18,31
L,19,32
L,20,33
L,21,34
L,22,35
L,23,36
L,24,37
L,25,38
L,26,39
L,27,28
L,28,29
L,29,30
L,30,31
L,31,32
L,32,33
L,33,34
L,34,35
L,35,36
L,36,37
L,37,38
L,38,39
csys,11
L,40,41
L,41,42
L,43,44
L,44,45
csys,12
L,46,47
L,47,48
L,48,49
L,49,46
csys,13
L,50,51
L,51,52
L,52,53
L,53,50
csys,14
L,54,55
L,55,56
csys,1
a,1,2,5
a,2,3,6
a,3,4,7
a,1,5,45
a,2,49,5
a,2,6,49
a,3,53,6
a,3,7,53
a,4,56,7
a,5,8,44,45
a,5,9,16,8
a,5,49,48,9
a,6,10,46,49
a,6,11,20,10
a,6,53,52,11
a,7,12,50,53
a,7,13,24,12
a,7,56,55,13
a,43,44,15,14
a,44,8,16,15
a,9,48,17,16
a,48,47,18,17
a,46,19,18,47
a,46,10,20,19
a,52,21,20,11
a,51,22,21,52
a,51,50,23,22
a,50,12,24,23
a,13,55,25,24
a,55,54,26,25
a,14,15,28,27
a,15,16,29,28
a,16,17,30,29
a,17,18,31,30
a,18,19,32,31
a,19,20,33,32
a,20,21,34,33
a,21,22,35,34
a,22,23,36,35
a,23,24,37,36
a,24,25,38,37
a,25,26,39,38
a,40,41,44,43
a,41,42,45,44
vext,1,44,1,,,.2

! Meshing, Loads and BC's
vmesh,all
vsel,s,volu,,31,42
nslv,s,1
nsel,r,loc,z,0,0
d,all,all,0
vsel,s,volu,,43,44
nslv,s,1
nsel,r,loc,z,.2,.2
sf,all,press,50000
csys
nsel,s,loc,x,0,0
dsym,symm,x
nsel,all
finish

! Solving
/solu
solve
finish
/post1
plnsol,s,x
```

APPENDIX B

ANSYS CODE FOR PRELOAD TEMPERATURE EFFECTS

```
!This File imports an IGES file, preloads
!the fastener, solves, resolves at 750 F

! Import IGES File from USB Drive
! Note: Drive in the IGESIN command
! may need to be updated to the location
! of the USB Drive
/Aux15
IOPTN,IGES,NODEFEAT
IOPTN,MERGE,YES
IOPTN,SOLID,YES
IOPTN,SMALL,YES
IOPTN,GTOLER, DEFA
IGESIN,'Wedge1641','IGS','F:\Thesis\A
nsys Thermal\'

/prep7
/title, Joint Analysis

! Create Volumes

nummrg,all
VA,55,56,57,58,59,60,61,62,63,64
FLST,2,14,5,ORDE,2
FITEM,2,65
FITEM,2,-78
VA,P51X
VA,79,80,81,82,83,84

! Material Properties, etc

et,1,92
mp,ex,1,4.64e7
mp,alpx,1,2.94e-6
mp,prxy,1,0.31
mp,ex,2,3.41e7
mp,alpx,2,6.8e-6
mp,prxy,2,0.295
mp,ex,3,2.35e7
mp,alpx,3,9.64e-6
mp,prxy,3,0.33
mp,ex,4,2.3e7
mp,alpx,4,4.28e-6
mp,prxy,4,0.337
tref,70

! Meshing

smrtsize,1
mat,1
vmesh,1
mat,2
vmesh,2
mat,3
vmesh,3
arefine,78,82,4,1

!Contact Pairs

!Under the Fastener Head - Standard
/COM, CONTACT PAIR CREATION -
START
CM,_NODECM,NODE
CM,_ELEMCM,ELEM
CM,_KPCM,KP
CM,_LINECM,LINE
CM,_AREACM,AREA
CM,_VOLUCM,VOLU
```

```
/GSAV,cwz,gsav,,temp
MP,MU,1,
MAT,1
R,3
REAL,3
ET,2,170
ET,3,174
KEYOPT,3,9,0
KEYOPT,3,10,2
R,3,
RMORE,
RMORE,,0
RMORE,0
! Generate the target surface
ASEL,S,,,59
CM,_TARGET,AREA
TYPE,2
NSLA,S,1
ESLN,S,0
ESLL,U
ESEL,U,ENAME,,188,189
ESURF
CMSEL,S,_ELEMCM
! Generate the contact surface
ASEL,S,,,78
CM,_CONTACT,AREA
TYPE,3
NSLA,S,1
ESLN,S,0
ESURF
ALLSEL
ESEL,ALL
ESEL,S,TYPE,,2
ESEL,A,TYPE,,3
ESEL,R,REAL,,3
/PSYMB,ESYS,1
/PNUM,TYPE,1
/NUM,1
EPLOT
ESEL,ALL
ESEL,S,TYPE,,2
ESEL,A,TYPE,,3
ESEL,R,REAL,,3
CMSEL,A,_NODECM
CMDEL,_NODECM
CMSEL,A,_ELEMCM
CMDEL,_ELEMCM
CMSEL,S,_KPCM
CMDEL,_KPCM
CMSEL,S,_LINECM
CMDEL,_LINECM
CMSEL,S,_AREACM
CMDEL,_AREACM
CMSEL,S,_VOLUCM
CMDEL,_VOLUCM
/GRES,cwz,gsav
CMDEL,_TARGET
CMDEL,_CONTACT
/COM, CONTACT PAIR CREATION -
END


!*
!Top of WTS - standard
/COM, CONTACT PAIR CREATION -
START
CM,_NODECM,NODE
CM,_ELEMCM,ELEM
CM,_KPCM,KP
CM,_LINECM,LINE
CM,_AREACM,AREA
CM,_VOLUCM,VOLU
/GSAV,cwz,gsav,,temp
MP,MU,1,0
MAT,1
R,5
REAL,5
ET,6,170
ET,7,174
KEYOPT,7,9,0
KEYOPT,7,10,2
R,5,
RMORE,
RMORE,,0
RMORE,0
! Generate the target surface
ASEL,S,,,57
CM,_TARGET,AREA
TYPE,6
NSLA,S,1
ESLN,S,0
ESLL,U
```

```
ESEL,U,ENAME,,188,189
ESURF
CMSEL,S,_ELEMCM
! Generate the contact surface
ASEL,S,,,65
CM,_CONTACT,AREA
TYPE,7
NSLA,S,1
ESLN,S,0
ESURF
ALLSEL
ESEL,ALL
ESEL,S,TYPE,,6
ESEL,A,TYPE,,7
ESEL,R,REAL,,5
/PSYMB,ESYS,1
/PNUM,TYPE,1
/NUM,1
EPLOT
ESEL,ALL
ESEL,S,TYPE,,6
ESEL,A,TYPE,,7
ESEL,R,REAL,,5
CMSEL,A,_NODECM
CMDEL,_NODECM
CMSEL,A,_ELEMCM
CMDEL,_ELEMCM
CMSEL,S,_KPCM
CMDEL,_KPCM
CMSEL,S,_LINECM
CMDEL,_LINECM
CMSEL,S,_AREACM
CMDEL,_AREACM
CMSEL,S,_VOLUCM
CMDEL,_VOLUCM
/GRES,cwz,gsav
CMDEL,_TARGET
CMDEL,_CONTACT
/COM, CONTACT PAIR CREATION -
END

! Outer Rim - standard
/COM, CONTACT PAIR CREATION -
START
CM,_NODECM,NODE
CM,_ELEMCM,ELEM
CM,_KPCM,KP
CM,_LINECM,LINE
CM,_AREACM,AREA
CM,_VOLUCM,VOLU
/GSAV,cwz,gsav,,temp
MP,MU,1,0
MAT,1
R,4
REAL,4
ET,4,170
ET,5,174
KEYOPT,5,9,0
KEYOPT,5,10,2
R,4,
RMORE,
RMORE,,0
RMORE,0
! Generate the target surface
ASEL,S,,,56
CM,_TARGET,AREA
TYPE,4
NSLA,S,1
ESLN,S,0
ESLL,U
ESEL,U,ENAME,,188,189
ESURF
CMSEL,S,_ELEMCM
! Generate the contact surface
ASEL,S,,,67
CM,_CONTACT,AREA
TYPE,5
NSLA,S,1
ESLN,S,0
ESURF
ALLSEL
ESEL,ALL
ESEL,S,TYPE,,4
ESEL,A,TYPE,,5
ESEL,R,REAL,,4
/PSYMB,ESYS,1
/PNUM,TYPE,1
/NUM,1
EPLOT
ESEL,ALL
ESEL,S,TYPE,,4
ESEL,A,TYPE,,5
```

```
ESEL,R,REAL,,4
CMSEL,A,_NODECM
CMDEL,_NODECM
CMSEL,A,_ELEMCM
CMDEL,_ELEMCM
CMSEL,S,_KPCM
CMDEL,_KPCM
CMSEL,S,_LINECM
CMDEL,_LINECM
CMSEL,S,_AREACM
CMDEL,_AREACM
CMSEL,S,_VOLUCM
CMDEL,_VOLUCM
/GRES,cwz,gsav
CMDEL,_TARGET
CMDEL,_CONTACT
/COM, CONTACT PAIR CREATION - END

! Loads and BC's

/pnum,mat,3
eplot
!psmesh,12,preload,,volu,3,0,y,0,,,,npts
!CM,PL,LINE
FLST,2,7,5,ORDE,7
FITEM,2,55
FITEM,2,62
FITEM,2,-63
FITEM,2,65
FITEM,2,76
FITEM,2,-77
FITEM,2,84
DA,P51X,SYMM
da,74,uy
!SLOAD,ALL,9,LOCK,FORC,250, 1,2
eqslve,pcg,1e-8,2
!cmplot
FINISH

! Solving Preload Model

/solu
nsub,1,1,1
solve

/post1
plnsol,s,y

! Raising Temperature to 750 F

/solu
antype,,restart
tunif,750

/title,Preload Analysis at 750 F

solve

/post1
plnsol,s,y
```

APPENDIX C

MTS TEST PROGRAM FOR FASTENER TENSILE TESTING

MPT PROCEDURE PARAMETERS - F:\mpt\Procs\FFtensile.000 12/14/09 3:52:08 PM
Items preceded by an asterisk (*) have been modified.

Application Information
  Name : MultiPurpose TestWare (MPT)
  Version : 3.3B 1205

Station Information
  Path :
  Configuration : 5.5kipFrameNo ACS.cfg
  Parameter Set : default

Procedure: FFtensile.000
  Sequencing
    Procedure is done when : Ramp to zero.Done

  Procedure / Ramp to start: Segment Command
    Sequencing
      Start : <Procedure>.Start
      Interrupt : None
    General
      Process Enabled : True
      Execute Process : 1 Time(s)
      Counter Type : None
    Command
      Segment Shape : Ramp
      Time : 5.0000 (Sec)
      Adaptive Compensators : None
      Do Not Update Counters : False
      Relative End Level : False
    Channels
      Axial
        Control Mode : Force
        Absolute End Level : 5.0000 (lbf)

Procedure / Testing: Segment Command
  Sequencing
    Start : Ramp to start.Done
    Interrupt : None
  General
    Process Enabled : True
    Execute Process : 1 Time(s)
    Counter Type : None
  Command
    Segment Shape : Ramp
    Time : 240.00 (Sec)
    Adaptive Compensators : None
    Do Not Update Counters : False
    Relative End Level : True
  Channels
    Axial
      Control Mode : Displacement
      Relative End Level : 0.07000 (in)

Procedure / Force Limits: Data Limit Detector
  Sequencing
    Start : <Procedure>.Start
    Interrupt : None
  General
    Process Enabled : True
    Execute Process : 1 Time(s)
    Counter Type : None
  Limits
    Axial Force
      Upper Limit : 3100.0 (lbf)
      Lower Limit : -40.0 (lbf)
  Settings
    Limit Mode : Absolute
    Process completes when : Any selected signal exceeds its limit
    Log Message As : Warning
    Action : Program Hold

Procedure / Displacement Limits: Data Limit Detector
  Sequencing
    Start : <Procedure>.Start
    Interrupt : None
  General
    Process Enabled : True
    Execute Process : 1 Time(s)
    Counter Type : None

Limits
Axial Displacement
Upper Limit : 0.1000 (in)
Lower Limit : -0.1000 (in)
Settings
Limit Mode : Relative
Process completes when : Any selected signal exceeds its limit
Log Message As : Warning
Action : Program Hold

Procedure / Daq: Timed Acquisition
Sequencing
Start : <Procedure>.Start
Interrupt : None
General
Process Enabled : True
Execute Process : 1 Time(s)
Counter Type : None
Acquisition
Time Between Points : 0.10010 (Sec)
Total Samples : Continuous sampling enabled
Signals
: Axial Force
: Axial Displacement
: Running Time
Destination
Buffer Size : 1024
Data Header :
Destination : Specimen data file
Buffer Type : Linear
Write First Data Header Only : False
Output Units
UAS : Current Unit AssigNment Set

Procedure / Failure Detector: Failure Detector
Sequencing
Start : <Procedure>.Start
Interrupt : None
General
Process Enabled : True
Execute Process : 1 Time(s)
Counter Type : None
Settings
Signal : Axial Force
Failure Event Percentage : 50.0
Failure Event Type : Maximum

```
    Initial Value                          : Absolute
    Sensitivity                            : 10.0 (lbf)
  Options
    Log Message As                         : Information
    Action                                 : Program Hold
  Destination
    Destination                            : Discard data
    Data Header                            :

Procedure / Ramp to zero: Segment Command
  Sequencing
    Start                                  : Testing.Done
    Interrupt                              : None
  General
    Process Enabled                        : True
    Execute Process                        : 1    Time(s)
    Counter Type                           : None
  Command
    Segment Shape                          : Ramp
    Time                                   : 30.000 (Sec)
    Adaptive Compensators                  : None
    Do Not Update Counters                 : False
    Relative End Level                     : False
  Channels
    Axial
      Control Mode                         : Force
      Absolute End Level                   : 0.00000 (lbf)

Execution Options
  Hold State Support                       : Enable Hold
  Resume Test After Stop                   : Enable Resume
  Required Power                           : High
  Command Hold Behavior                    : Stay at Level
  Command Stop Behavior                    : Taper to Zero
  Setpoint                                 : Disable and Reset
  Span                                     : Disable and Reset
  Confirm actions that may affect resuming the test       : True
Specimen Options
  Data File Mode                           : Append
  Data File Format                         : Excel
  Specimen Log Mode                        : Append
  Data File Time Stamp                     : Time
  Clear Counters on Reset                  : True
Recovery Options
  Enable saving recovery status:           : True
  Upon program state change                : True
```

At least every: : 60.000 (Sec)
Message Options
Message Capture
Minimum Severity : Information
Source : All Applications
Archive Auto Deletion
Delete Older Than : Disabled
Control Panel Display Options
Test Progress
Run Time : Display As HH:MM:SS
Counters
Channel Counters : Display As Cycles
Sequence Counters : Display As Cycles
Specimen
Procedure Name : True
Procedure State : True
Station Status
Power : True
Procedure Properties
Description :
Author :
Unit Selection
Current UAS : Use Station Unit AssigNment Set

APPENDIX D

MTS TEST PROGRAM FOR FASTENER FATIGUE TESTING

MPT PROCEDURE PARAMETERS - F:\mpt\Procs\FFCyclicDaq.000 12/10/09 2:23:24 PM
Items preceded by an asterisk (*) have been modified.

Application Information
  Name : MultiPurpose TestWare (MPT)
  Version : 3.3B 1205

Station Information
  Path :
  Configuration : 5.5kipFrameNo ACS.cfg
  Parameter Set : default

Procedure: FFCyclicDaq.000
  Sequencing
    Procedure is done when : Cycling.Done

  Procedure / Ramp to start: Segment Command
    Sequencing
      Start : <Procedure>.Start
      Interrupt : None
    General
      Process Enabled : True
      Execute Process : 1 Time(s)
      Counter Type : None
    Command
      Segment Shape : Ramp
      Time : 5.0000 (Sec)
      Adaptive Compensators : None
      Do Not Update Counters : False
      Relative End Level : False
    Channels
      Axial
        Control Mode : Force
        Absolute End Level : 81.000 (lbf)

Procedure / Cycling: Cyclic Command
  Sequencing
    Start : Ramp to start.Done
    Interrupt : None
  General
    Process Enabled : True
    Execute Process : 1 Time(s)
    Counter Type : None
  Command
    Segment Shape : Sine
    Frequency : 40.000 (Hz)
    Count : Continuous cycling enabled
    Adaptive Compensators : PVC
    Do Not Update Counters : False
    Relative End Levels : False
  Channels
    Axial
      Control Mode : Force
      Absolute End Level 1 : 81.000 lbf
      Absolute End Level 2 : 452.00 lbf
      Phase Lag : 0.00 (deg)

Procedure / Force Limits: Data Limit Detector
  Sequencing
    Start : <Procedure>.Start
    Interrupt : None
  General
    Process Enabled : True
    Execute Process : 1 Time(s)
    Counter Type : None
  Limits
    Axial Force
      Upper Limit : 2000.0 (lbf)
      Lower Limit : -20.0 (lbf)
  Settings
    Limit Mode : Absolute
    Process completes when : Any selected signal exceeds its limit
    Log Message As : Warning
    Action : Program Hold

Procedure / Displacement Limits: Data Limit Detector
  Sequencing
    Start : <Procedure>.Start
    Interrupt : None
  General

Process Enabled : True
Execute Process : 1 Time(s)
Counter Type : None
Limits
Axial Displacement
Upper Limit : 0.2000 (in)
Lower Limit : -0.2000 (in)
Settings
Limit Mode : Relative
Process completes when : Any selected signal exceeds its limit
Log Message As : Warning
Action : Program Hold

Procedure / Cyclic DAQ: Cyclic Acquisition
Sequencing
Start : Ramp to start.Done
Interrupt : None
General
Process Enabled : True
Execute Process : 1 Time(s)
Counter Type : None
Cycles
Master Channel : Axial
Data Storage Pattern : Logarithmic (1,2,3,4,5,6,7,8,9)
Relative Cycle or Segment Counts : False
Maximum Cycle Stored : 200000000 (cycle)
Store Data At : 1.0, 2.0, 3.0, 4.0, 5.0, 6.0, 7.0,
: 8.0, 9.0, 10.0, 20.0, 30.0, 40.0,
: 50.0, 60.0, 70.0, 80.0, 90.0, 100.0,
: 200.0, 300.0, 400.0, 500.0, 600.0,
: 700.0, 800.0, 900.0, 1000.0, 2000.0,
: 3000.0, 4000.0, 5000.0, 6000.0, 7000.0,
: 8000.0, 9000.0, 10000.0, 20000.0,
: 30000.0, 40000.0, 50000.0, 60000.0,
: 70000.0, 80000.0, 90000.0, 100000.0,
: 200000.0, 300000.0, 400000.0, 500000.0,
: 600000.0, 700000.0, 800000.0, 900000.0,
: 1000000.0, 2000000.0, 3000000.0,
: 4000000.0, 5000000.0, 6000000.0,
: 7000000.0, 8000000.0, 9000000.0,
: 10000000.0, 20000000.0, 30000000.0,
: 40000000.0, 50000000.0, 60000000.0,
: 70000000.0, 80000000.0, 90000000.0,
: 100000000.0, 200000000.0 (cycle)
Store Data For : 5 (segments)
Acquisition

```
    Acquisition Method                          : Peak/Valley
    Peak/Valley Signal                          : Axial Force
    Peak/Valley Sensitivity                     : 50.0 (lbf)
  Signals
                                                : Axial Segment Count
                                                : Axial Force
                                                : Axial Displacement
                                                : Running Time
  Destination
    Data Header                                 :
    Write First Data Header Only                : True
    Destination                                 : Specimen data file
  Output Units
    UAS                                         : Current Unit AssigNment Set

Procedure / Min/Max DAQ: Max/Min Acquisition
  Sequencing
    Start                                       : Ramp to start.Done
    Interrupt                                   : None
  General
    Process Enabled                             : True
    Execute Process                             : 1   Time(s)
    Counter Type                                : None
  Acquisition
    Master Signal                               : Axial Force
    Maximum Values                              : True
    Minimum Values                              : True
  Signals
                                                : Axial Force
                                                : Axial Displacement
                                                : Axial Segment Count
  Destination
    Data Header                                 : Max/ Min Data
    Destination                                 : Specimen data file
  Output Units
    UAS                                         : Current Unit AssigNment Set

Execution Options
  Hold State Support                            : Enable Hold
  Resume Test After Stop                        : Enable Resume
  Required Power                                : High
  Command Hold Behavior                         : Stay at Level
  Command Stop Behavior                         : Taper to Zero
  Setpoint                                      : Disable and Reset
  Span                                          : Disable and Reset
  Confirm actions that may affect resuming the test       : True
```

Specimen Options
  Data File Mode : Append
  Data File Format : Excel
  Specimen Log Mode : Append
  Data File Time Stamp : Time
  Clear Counters on Reset : True
Recovery Options
  Enable saving recovery status: : True
  Upon program state change : True
  At least every: : 60.000 (Sec)
Message Options
  Message Capture
    Minimum Severity : Information
    Source : All Applications
  Archive Auto Deletion
    Delete Older Than : Disabled
Control Panel Display Options
  Test Progress
    Run Time : Display As HH:MM:SS
  Counters
    Channel Counters : Display As Cycles
    Sequence Counters : Display As Cycles
  Specimen
    Procedure Name : True
    Procedure State : True
  Station Status
    Power : True
Procedure Properties
  Description :
  Author :
Unit Selection
  Current UAS : Use Station Unit AssigNment Set

REFERENCES

[1] Redmond, P. E., 2006, "Failure Analysis Investigation of Two Sets of Broken Mechanical Fasteners," Southwest Research Institute, San Antonio

[2] Smith, D.F., Smith, J.S., and Floreen, S., 1984, "A Silicon-Containing, Low-Expansion Alloy with Improved Properties," *Superalloys 1984: Proceedings of the Fifth International Symposium on Superalloys,* Champion, Pa, **Vol. 5**, pp. 591-600.

[3] Coffin, L. F., Jr., 1977, "Fatigue at High Temperature," *Fracture 1977*, D. M. R. Taplin, ed., University of Waterloo Press, Waterloo, Ontario, Canada, **Vol. 1,** pp. 263-292.

[4] Sheffler, K.D., 1976, "Vacuum Thermal-Mechanical Fatigue Behavior of Two Iron-Base Alloys," Thermal Fatigue of Materials and Components, **ASTM STP 612**, pp. 214-226.

[5] Aerospace Industries Association of America, 1997,"Fastener Test Methods: Method 5 Stress Durability," NASM 1312-5, National Aerospace Standard

[6] Beer, F., et al, 2008, *Mechanics of Materials, 3rd Ed.,* McGraw-Hill, New York, pp. 815, Appendix C

[7] National Aeronautics and Space Administration, 1998, "Criteria for Preloaded Bolts", NSTS 08307 Revision A

[8] Budynas, R. G., Nisbett, J. K., 2008, *Shigley's Mechanical Engineering Design, 8th Ed.,* McGraw-Hill, New York, pp. 427.

[9] Bickford, J. H., 1995, *An Introduction to the Design and Behavior of Bolted Joints, 3rd Ed.*, Marcel Dekker, New York